AD-A155 017 BOREHOLE TILT MEASUREMENTS FROM CHARLEVOIX QUEBEC(U) 1/1
DALHOUSIE UNIV HALIFAX (NOVA SCOTIA) DEPT OF
OCEANOGRAPHY J A PETERS ET AL. MAR 84 AFGL-TR-84-0238
UNCLASSIFIED F19628-83-K-0023 F/G 8/7 NL

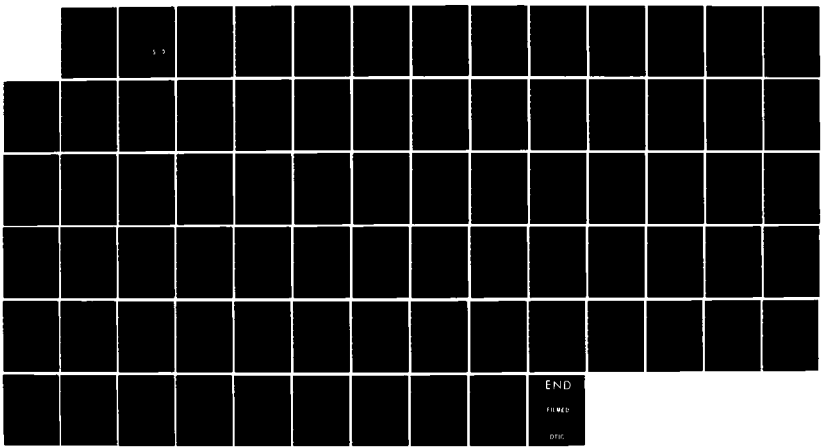

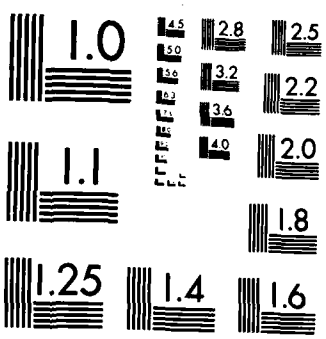

MICROCOPY RESOLUTION TEST CHART
NATIONAL BUREAU OF STANDARDS-1963-A

AD-A155 017

AFGL-TR-84-0238

BOREHOLE TILT MEASUREMENTS FROM CHARLEVOIX, QUEBEC

J.A. Peters
C. Beaumont

Oceanography Department
Dalhousie University
Halifax, Nova Scotia
Canada

Scientific Report No. 1

March 1984

DTIC
ELECTE
JUN 1 2 1985
S D
G

Approved for public release; distribution unlimited

AIR FORCE GEOPHYSICS LABORATORY
AIR FORCE SYSTEMS COMMAND
UNITED STATES AIR FORCE
HANSCOM AFB, MASSACHUSETTS 01731

DTIC FILE COPY

85 5 17 178

This report has been reviewed by the ESD Public Affairs Office (PA) and is releasable to the National Technical Information Service (NTIS).

This technical report has been reviewed and is approved for publication.

JOHN J. CIPAR
Contract Manager

HENRY A. OSSING, Chief
Solid Earth Geophysics Branch

FOR THE COMMANDER

DONALD H. ECKHARDT, Director
Earth Sciences Division

Qualified requestors may obtain additional copies from the Defense Technical Information Center. All others should apply to the National Technical Information Service.

If your address has changed, or if you wish to be removed from the mailing list, or if the addressee is no longer employed by your organization, please notify AFGL/DAA, Hanscom AFB, MA 01731. This will assist us in maintaining a current mailing list.

Do not return copies of this report unless contractual obligations or notices on a specific document requires that it be returned.

Unclassified

SECURITY CLASSIFICATION OF THIS PAGE

AD-A155 017

REPORT DOCUMENTATION PAGE

1a. REPORT SECURITY CLASSIFICATION Unclassified	1b. RESTRICTIVE MARKINGS
2a. SECURITY CLASSIFICATION AUTHORITY	3. DISTRIBUTION/AVAILABILITY OF REPORT Approved for public release; distribution unlimited
2b. DECLASSIFICATION/DOWNGRADING SCHEDULE	
4. PERFORMING ORGANIZATION REPORT NUMBER(S)	5. MONITORING ORGANIZATION REPORT NUMBER(S) AFGL-TR-84-0238
6a. NAME OF PERFORMING ORGANIZATION Oceanography Department Dalhousie University 6b. OFFICE SYMBOL (If applicable)	7a. NAME OF MONITORING ORGANIZATION
6c. ADDRESS (City, State and ZIP Code) Halifax, Nova Scotia Canada	7b. ADDRESS (City, State and ZIP Code)
8a. NAME OF FUNDING/SPONSORING ORGANIZATION Air Force Geophysics Laboratory 8b. OFFICE SYMBOL (If applicable) LWH	9. PROCUREMENT INSTRUMENT IDENTIFICATION NUMBER F19628-83-K-0023
8c. ADDRESS (City, State and ZIP Code) Hanscom AFB, Massachusetts 01731 Monitor/John J.Cipar	10. SOURCE OF FUNDING NOS. PROGRAM ELEMENT NO.: 61102F; PROJECT NO.: 2309; TASK NO.: G2; WORK UNIT NO.: AN
11. TITLE (Include Security Classification) Borehole Tilt Measurements From Charlevoix,Quebec	
12. PERSONAL AUTHOR(S) J.A.Peters and C.Beaumont	
13a. TYPE OF REPORT Sci Rpt No.1 13b. TIME COVERED FROM ____ TO ____	14. DATE OF REPORT (Yr., Mo., Day) 1984 March 15. PAGE COUNT 75
16. SUPPLEMENTARY NOTATION	

17. COSATI CODES			18. SUBJECT TERMS (Continue on reverse if necessary and identify by block number)
FIELD	GROUP	SUB. GR.	Geophysics Earth Tides Tiltmeters

19. ABSTRACT (Continue on reverse if necessary and identify by block number)

An array of three borehole tiltmeters near Quebec City in Eastern Canada is designed to study the tidal and secular response of the crust in the Charlevoix seismic zone. The objectives of this first study of data from two boreholes of the array are to investigate the spatial coherency of the tidal observations and determine whether there are time variations in the tidal amplitudes and phases; and to explore the main features of the secular tilt signal. The tidal analysis was done using a modified version of the HYCON harmonic analysis program of Schuller [1977], with which the time varying tidal amplitudes and phases were determined by the sequential analysis of overlapping 2 monthly subsets of the data. The admittance variations observed for the major constituents (M_2, N_2, S_2K_2, O_1, $P_1S_1K_1$) show remarkable agreement between boreholes, suggesting that they are regional in origin. Differences of up to 20% in amplitude and 5 degrees in phase were found between the mean M_2 results determned from boreholes 1 and 2, indicating small-scale distortion of the local tilt field by lateral inhomogeneities. The secular tilt from both boreholes

20. DISTRIBUTION/AVAILABILITY OF ABSTRACT UNCLASSIFIED/UNLIMITED ☒ SAME AS RPT ☐ DTIC USERS ☐	21. ABSTRACT SECURITY CLASSIFICATION Unclassified
22a. NAME OF RESPONSIBLE INDIVIDUAL John J. Cipar	22b. TELEPHONE NUMBER (Include Area Code) (617)861-3746 22c. OFFICE SYMBOL LWH

DD FORM 1473, 83 APR EDITION OF 1 JAN 73 IS OBSOLETE.

SECURITY CLASSIFICATION OF THIS PA

CONTINUED FROM BLOCK 19:

correlates strongly with transient and seasonal water table fluctuations, suggesting the dominant influence of pore pressure effects on the non-tidal tilt. A preliminary estimate of the detectability of long term regional trends in tilt is 0.4 μrad/yr.

Accession For
NTIS GRA&I
DTIC TAB
Unannounced
Justification
By
Distribution/
Availability Codes
Dist | Avail and/or Special
A/1

ABSTRACT

An array of three borehole tiltmeters near Québec City in Eastern Canada is designed to study the tidal and secular response of the crust in the Charlevoix seismic zone. The objectives of this first study of data from two boreholes of the array re to investigate the spatial coherency of the tidal observations and determine whether there are time variations in the tidal amplitudes and phases; and to explore the main features of the secular tilt signal. The tidal analysis was done using a modified version of the HYCON harmonic analysis program of Schuller [1977], with which the time varying tidal amplitudes and phases were determined by the sequential analysis of overlapping 2 monthly subsets of the data. The admittance variations observed for the major constituents (M_2, N_2, S_2K_2, O_1, $P_1S_1K_1$) show remarkable agreement between boreholes, suggesting that they are regional in origin. Differences of up to 20% in amplitude and 5 degrees in phase were found between the mean M_2 results determined from boreholes 1 and 2, indicating small-scale distortion of the local tilt field by lateral inhomogeneities. The secular tilt from both boreholes correlates strongly with transient and seasonal water table fluctuations, suggesting the dominant influence of pore pressure effects on the non-tidal tilt. A preliminary estimate of the detectability of long term regional trends in tilt is 0.4 μrad/yr.

1. INTRODUCTION.

An array of three borehole tiltmeters has been established in the Charlevoix region of Québec (figure 1), an area considered to be among the most seismically active in eastern North America. The tilt observations are being made at the Charlevoix Geophysical Observatory of the Canadian Department of Energy, Mines and Resources and are aimed at investigating the behaviour of crustal rocks in an earthquake zone. Specifically, the program of measurements is designed to sample the earth tide response as a possible indicator of changing crustal conditions and, by monitoring secular and transient tilts, to directly detect regional crustal deformations associated with processes occurring at depth.

This first analysis of the borehole tilt data from the Charlevoix Observatory provides an explanation of the first order properties of the secular tilt, establishes a methodology for determining the real variations in the tidal admittance, and applies this approach to the Charlevoix data. On the basis of our results we then assess the potential of using the time varying tidal admittance at Charlevoix as an indicator of changes in crustal response; and of using the secular component to detect long term tilts of tectonic origin.

The first study of tidal response in relation to earthquake activity was reported by Nishimura [1950] who recorded fluctuations of up to 75% in monthly amplitude determinations of the M_2 constituent using quartz pendulums installed 165m below ground in Makimine copper mine,

Japan. These variations were attributed to elastic parameter changes in the local crust modifying the tidal response. It was suggested that the longer term changes in the tidal amplitudes were correlated with fluctuations in seismic activity. Other studies have indicated less dramatic effects, the measured tidal response variations generally not exceeding 15%. Kato [1979] measured 2-4% amplitude fluctuations in M_2 from observations recorded by a water tube tiltmeter at Kamitakara during September, 1977 to October, 1978. Monthly M_2 strain amplitudes at the same location from 1968 to 1972 [Mikumo et al, 1978] showed a steady rise of 15% during the eleven months prior to the 1969 Gifu (M=6.6) earthquake. More recent results from the Makimine station [Tanaka, 1976] indicated amplitude variations not exceeding a range of 20%; and it has been suggested that the extraordinary amplitude changes seen by Nishimura [1950] included instrumental effects. Agnew [1979] has studied the time variation of M_2 in strain data recorded on the 800m laser strainmeter at Piñon Flat, California. From 1973 to 1978 fluctuations were confined within 2% of the mean amplitude. Given the high signal to noise ratio (45dB) of the estimates and the fact that Piñon Flat is locally an aseismic region, this result establishes an experimental baseline upon which to evaluate the significance of time variations in admittance in active seismic zones.

Beaumont and Berger [1974] suggested that if V_p/V_s seismic velocity anomalies are indicative of changes in crustal elastic properties, then they should be accompanied by tidal response anomalies. For tilt, this would be caused by a laterally varying effect where, for example,

a 15% reduction in V_p within a crustal inclusion would be accompanied by a maximum 30-40% change in amplitude at the edge of the inclusion, decreasing rapidly with distance away from it. Tanaka [1976] has used a similar approach to look at the modification of the marine load tide response due to a dilatant zone near the coast. Beaumont [1978a] expanded on the work of Beaumont and Berger [1974] by considering the effect on the tidal response of the superposition of tidal and increasing tectonic stress regimes in the crust. Appealing to laboratory results which showed that hysteresis occurs in intact rock samples as they approach failure, he outlined ways in which linear and non-linear anomalies in the tidal response may be generated depending on the rate of change of stress in the crust. Agnew [1981] extended the theoretical analysis further considering different types of non-linearities and searched for their signature in strain records at Piñon Flat without success.

There is a catalogue of attempts to measure tectonic tilts and strains in the non-tidal part of the spectrum (see, for example, Wyatt et al [1982]; McConnell and Lewkowicz [1978]; Herbst [1976]; Mortensen and Johnston [1975]). Few have been demonstrably successful, for the most part because such measurements are carried out near the surface where they are severely polluted by other, inseparable signals usually of meteorological origin. It is clear that any hope of success lies in an approach which either ensures the isolation of the measurement from these sources of noise (by deep enough burial) or one which entails a spatial average of the near surface signal. This second approach may

involve a network of instruments and subsequent statistical elimination of noise [Mortensen and Johnston, 1975], or the use of long baseline instruments [Wyatt et al, 1982]. These methods assume that the spatial scales of the meteorological and other sources of noise are less than that of true tectonic tilt anomalies. Wyatt et al [1982] in an important comparative experiment at Piñon Flat, demonstrated the relative potential for secular tilt studies of measurements performed over a long baseline (535m), at moderate depth (26m), and in shallow (5m) borehole installations. Their results, for data spanning a 5 month period, indicate successive order of magnitude increases in the drift rates from the long baseline tiltmeter (0.07 μrad/month) to the 26m deep borehole tiltmeter (0.4 μrad/month) to the shallow installations (up to 7 μrad/month). However, the most encouraging results to date are those of Cabaniss [1978] who achieved a net secular drift of 0.3 μrad in a 120m deep borehole at Bedford, Massachussetts over a three year period.

The Charlevoix region has a history of large earthquakes occurring roughly every 60 to 90 years. The last major earthquake was a magnitude 7 which struck in 1925. Seismicity surveys in 1968, 1970 and 1974 [Milne et al, 1970; Leblanc et al, 1973; Leblanc and Buchbinder, 1977] show that the earthquake zone covers a 70 by 40 Km region centred on the St. Lawrence River 150 Km northeast of Québec City. Almost all of the earthquakes were shown to have occurred within the Precambrian rocks of the Grenville Province, at an average depth of 11 Km. The nodal plane solutions are compatible with pure thrusting, the planes

dipping on average 40 degrees to the west and 50 degrees to the east [Leblanc and Buchbinder, 1977] with the direction of the pressure axis not in disagreement with what Sbar and Sykes [1973] found in other parts of North America. Overlying the Grenville basement rocks are the Ordovician sediments deposited during the Taconic orogeny. During the 1974 survey no events were detected above the contact between the basement and sediments, which outcrops at Logan's Line along the north shore of the river. It appears, on the basis of this measured distribution, that the length of the seismic zone parallel to the river is related to the 350Ma old Charlevoix impact crater [Robertson, 1968; 1975] (see figure 1). The conjunction of Logan's Line and the crater could influence the seismicity distribution [Leblanc et al, 1973; Leblanc and Buchbinder, 1977]. Presumably, the structures either represent a zone of weakness, remaining from crustal damage caused during the impact, in which tectonic stress is released by earthquakes, or the structures focus the tectonic stress in some way causing a higher rate of seismicity in an otherwise normal crust.

Seismic crustal studies [Lyons et al, 1980] indicate that the Ordovician overthrusts dip beneath the river southeast of Logan's Line at an average of 20 degrees. Their results also indicate that the upper crustal seismic P-velocity in a belt extending along the north shore of the river is 0.2-0.3 Km/sec lower than the average 6.4-6.5 Km/sec for the Grenville Province. They suggest that this is related to structural deformation caused by the Charlevoix meteorite impact. The near surface P-velocity within the crater is 6.08 Km/sec suggestive of a zone weak-

ened by fracturing during impact.

Since 1972 various kinds of geophysical measurements have been made by the Earth Physics Branch of the Department of Energy, Mines and Resources to supplement the existing horizontal and vertical control provided by the Geological Survey of Canada. Thus, at the present time the geophysical measurements in the area [Buchbinder et al, in press] comprise: 1) first order levelling along the north and south shores of the St. Lawrence River; 2) a precise gravity network consisting of 15 stations and twenty-two connections; 3) a triangulation network consisting of twelve points and twenty-six connections spanning the St. Lawrence River; 4) two permanent tide gauges; 5) a permanent seismic observatory at La Pocatière on the south shore; 6) an array of four magnetotelluric stations; and 7) tilt, strain, seismic and magnetotelluric installations located at the Charlevoix Observatory and operating in conjunction with borehole tiltmeter programme to be discussed in this study.

In the following sections, we describe briefly the experimental set-up and discuss in detail the methods and procedures used in analysing the tilt data. Particular attention is paid to the elimination of apparent time variations in the admittance which are artifacts of the analysis. It is shown that while the mean admittances for the M_2 and O_1 tidal constituents are in poor agreement between boreholes, there is good agreement between the boreholes for the identified real time changes in admittance. Quasi-periodic variations in the M_2 constituent, indicating an approximately six monthly cycle, reach a level of

5% in amplitude and 3-4 degrees in phase. Non-tidal tilts in the observed data are at the level of 1-2 μrad and are strongly correlated with groundwater level. Incoherent residual drifts appear to be present at a minimum level of 0.4 μrad/yr.

2. THE BOREHOLE TILTMETER ARRAY

The tiltmeter borehole array consists of three 30cm diameter holes, two of which are 46m deep (boreholes 1 and 2) and the third (borehole 3) which is 110m deep [Peters, 1983]. Each is cased with a 20cm diameter mild steel casing terminated by a 6m long stainless steel pod of the same diameter which houses the tiltmeter. All of the holes are dry, but only the shorter two are straight. *Figure 2 is a diagram* of the experimental configuration, showing a plan view of the observatory, and the tiltmeter installation in section. Adjacent to each of the boreholes is a well (referred to as A, B or C) in which manual and continuous measurements of water level are made. A vault containing three ANAC mercury level tiltmeters is situated near the centre of the borehole array [Peters et al, 1983].

The borehole tiltmeters are Bodenseewerk Gbp 10 (formally Askania) vertical pendulums [Flach and Rosenbach, 1971] chosen because of their proven performance [Zschau, 1976; Edge et al, 1979;1983; Flach et al, 1975] and, not least, because they are the only high quality tiltmeters commercially available and supported. The most important feature of the instrument is the accurate in situ calibration absent in most other

ions between 105 and 107, operating at different times in borehole 1, exceeds the range of variability so far determined. The averaged ANAC results do, however, plot between the borehole 1 observations. Tiltmeter 106 in borehole 2 lags the other measurements by 4-5 degrees in the south direction and leads by nearly 7 degrees in the east direction. Furthermore, there is a 20% difference between the 106 and 107 amplitudes in the east. The O_1 results are in fairly good agreement. A detailed examination of the coherency of a number of constituents [Peters and Kumpel, in prep] has confirmed that the large discrepancies between the two boreholes for some of the constituents is a real effect rather than instrumental.

While there is general agreement between theory and the observed O_1 admittances, there are systematic differences between all of the M_2 measurements and theory. In both directions, observations lag the model results. In the south, where drying is important, the observed amplitudes lie within the range of the total drying (3) and non-drying (4) model vectors and may constrain the model to the partial drying case which is midway between the two extremes and is physically the most realistic. Nevertheless, the layered earth model used to compute the tilt Green's functions does not take into account the regional structure dominated by Logan's contact (section 1) nor are corrections made for the effects of local topography and geological structure.

5.4 Time variations in the tidal constituents

One aspect of this study is to identify "true" variability, or

higher frequencies in Berger and Levine [1974]. Although the tilt spectra do not extend to high enough frequencies to show a conclusive trend, there is the suggestion of a similar increase in slope after 70 μHz at Charlevoix and Llanrwst. Also, there is a geographical relationship evident in the spectral characteristics. Those measurements which are most strongly influenced by marine loading effects (Queensbury, Llanrwst and Charlevoix) possess the highest background noise persisting over the entire spectrum. It is apparent that in coastal locations the lower limits to ground noise are determined by dynamical effects in the oceans. It is not clear whether this is also the case for inland sites.

5.3 Comparison of observed and theoretical tidal tilts

Figure 12 shows polar diagrams of the observed and computed M_2 and O_1 mean admittances for: tiltmeters 105 and 107 (borehole 1); tiltmeter 106 (borehole 2); and the ANAC measurements A/D and C/D [Peters et al, 1983] made in the shallow vault (figure 2). Also shown are the loading model results based on the computations outlined in section 4. Peters et al [1983] concluded that due to the geometry of the vault and the expected strain-tilt coupling effects, the ANAC measurements are best approximated by the average of the two measurements. An error of 180 degrees in the phase of the ANAC D component quoted in Peters et al [1983] has been corrected.

There are substantial differences in the observed M_2 results among all of the measurements. A 5-8% amplitude discrepancy in both direct-

The main difference between the spectra is in the power associated with the 4th and 6th diurnal bands. In both cases the level in the south component is ten times smaller than in the east component. This difference is surprising since the large marine tide and the substantial drying areas in the estuary to the south of the site are expected to be a rich source of higher harmonics in the marine tides. Peters and Kumpel [in prep] show that the non-linear tilt signal can be explained by loading of the marine tides and that the large difference between the component directions is due to the spatial distribution of these shallow water constituents.

It is interesting to compare the residual background noise, after removal of the tides, among different measurements which cover a range of techniques and geographical locations. In figure 11, we compare the published background noise spectra from three strain and four tilt measurements, including that of 107 east from borehole 1 (see figure caption for details). The spectra are plotted on a log-log scale and all show the characteristic "red noise" linear trend typical of geophysical spectra plotted in this way. Interestingly, the slopes among the strain spectra, and among three of the tilt spectra, are remarkably consistent. In the case of strain, the relationship between noise power, P, and frequency, f, is $P \propto f^{-2.9}$. For each of the tilt measurements, $P \propto f^{-2.3}$, excepting Llanrwst where the noise level decays more slowly. There is evidence that these slopes change between the frequencies 50 and 500 μHz. This is clear for the Queensbury strain spectrum, and also for the Piñon Flat and Poorman strain spectra plotted to

eted. The origin of this component of the long term tilt is not known. A more detailed study of these and shorter period hydrologically induced tilts is in progress [Kumpel and Peters, in prep] using continuous water level data. Theoretical results [Kumpel, in prep] suggest that tilts of the observed size can be induced by pore pressure changes that occur in the rock matrix.

5.2 Power spectrum of the residual time series

The accuracy of the tidal estimates depends upon the residual energy in the tidal bands. Before discussing the tidal results, we will examine the residual power spectra of the ensemble average (section 3.3) shown in figure 10 for both components of tiltmeters 106 and 107.

The residuals in all components share a number of common features. Firstly, there is a strong presence of quarter, sixth and tenth diurnal energy, presumably generated by shallow water non-linear interactions from the marine load signal. Otherwise, the spectra consist of a statistically featureless background which decreases in power with increasing frequency but flattens out beyond 70 μHz (6 cycles/day) at a level of 0.025 $nrad^2/\mu Hz$ (power spectral density). Lastly, there is a distinct "hole" in the semi-diurnal band, as expected, where most of the energy has been removed in the least squares analysis for the tidal constituents. However, there is also significant residual energy, more prominent in 106, remaining in that band, suggesting that the linear tidal model cannot account for all of the signal.

100 degree azimuth during the second period correlates closely with the water level changes. If it is assumed that water level changes cause the secular tilt, a 40 degree difference in the direction of the water level effect in two boreholes 80m apart is not really surprising. On the evidence from drilling operations, the formation permeability is likely to be fracture dominated and there is no reason to expect a uniform fracture distribution or orientation over distances of the order of 80m.

The amplitude of the tilt induced by the water level changes is different for each borehole. For 105 in borehole 1, the large spring water level transient yielded 0.4 μrad per metre of water level change. Tiltmeter 107 in the same borehole gave 0.35 μrad per metre for the April event and 0.5 μrad per metre for the November event. Tiltmeter 106 in borehole 2 was, however, nearly twice as sensitive on both occasions, giving 0.65 μrad per metre and 0.8 μrad per metre in April and November, respectively. Again, it is not surprising that in an area of fracture dominated permeability, water level induced tilts are varying on a scale of 80m since the fractures in the immediate vicinity of the boreholes are expected to dominate the response.

There is a very clear monotonic drift in 107 of 1.2 μrad to the north-east (θ = 45 degrees) in addition to the first order (θ = 135 degrees) cyclical effect that correlates with the water level. There is evidence of a similar but smaller trend in 106, although the direction may be reversed. The sense of the residual drift in the case of 105 is not certain because the annual water level related cycle was not compl-

5. RESULTS

5.1 Correlation of secular tilt with water level changes

Figures 8(a) and 8(b) show the low pass filtered observations (sampled every 48 hours) for tiltmeter 105 operating in borehole 1 during 1980/1 and tiltmeters 106 and 107 operating concurrently in boreholes 2 and 1 during 1981/2. Also shown are hand measured water level data observed in well B(70) near borehole 2. The east and south components of 105 behave very similarly, both in the short and the long term. The total range of the 105 drift in each direction over the 260 day interval is 1.5 μrad. Although the water level is not adequately sampled to show short term fluctuations, there is a strong long term correlation with the tilt. A similar correlation exists between water level and tilt for tiltmeters 106 and 107. Furthermore, the directions of highest correlation with water level change are similar for each of the boreholes. This can best be seen in the tilt trajectories plotted in figure 9. The predominant drift direction, θ, for 105 has an azimuth of 135 degrees and for 107, operating in the same borehole one year later, the drift azimuth is 145 degrees. The situation for 106 is more complicated. We believe that from the time of installation in 1981 to day 180 (June 29) of 1982, tiltmeter 106 was not well seated in the borehole. The drift signal during this time was large and, apart from the large water level related transient in April, bears little resemblance to the 107 signal. After day 180, 106 was reinstalled and from this time the drift signal was considerably smaller. The tilt in the

4. THE MARINE TIDAL LOADING MODEL

The load tilt calculations were made by the same method as those of Beaumont and Lambert [1972], Beaumont [1978b], and Beaumont and Boutilier [1978], assuming a uniform, spherical earth. Firstly, the Green's functions for the point load response of the earth model were computed. The integrated effect of the ocean tide distribution was found by convolving the Green's functions with the in-phase and quadrature components of the tidal distribution. The cotidal charts were divided into triangular areas in which the amplitude and phase of the tides could be regarded as constant in order that the convolution could be evaluated numerically [Bower, 1971]. A more detailed representation of the tides in the St. Lawrence estuary and Saguenay river (figure 5) was used here than in the earlier work because most of the load tilt is generated close to the Charlevoix Observatory. The cotidal charts (figures 6 and 7) for this region are empirical but are based on observations from the coastal sites indicated, and on numerical calculations of the M_2 and O_1 constituents [El-Sabh et al, 1979]. We suspect that the largest errors in the marine tidal loading model arise from areas that "dry" during the tidal cycle (outlined by the fine dashed lines in figure 6). For this reason the computation has been done for two extreme cases in which there is no drying and in which areas that dry remain permanently dry. Errors also arise from the non-stationarity and non-linearity of the tides.

3.3 Fourier Analysis of the Tidal Residuals

Power spectral analysis of the 106 and 107 tidal residuals was performed in order to determine an upper limit of the signal to noise ratio for the main tidal constituents. The Fourier transform with the Hanning window applied was calculated for 5 independent 2 month sets covering the 13 months of data studied. The power spectrum was computed for each set and the ensemble average calculated to increase the stability of the estimates.

With a view to examining the detailed spectral content of the tidal residuals, a high resolution Fourier amplitude spectrum was calculated, with the Hanning window applied, for the 106 and 107 residual time series, after subtracting the mean tidal estimates resulting from harmonic analysis of the 29 overlapping sample series. The amplitude spectrum was computed with a frequency resolution of 58.5nHz, corresponding to the fundamental frequency for the time series, at intervals of 30 nHz. Our main objective in this high resolution analysis was to identify unresolved and unaccounted for waves which possess enough energy to influence the major constituents in our two months analyses. We might expect that the culprits, if any, will be non-linear shallow water waves, for example OP_2 or MKS_2, which certainly do not have the same admittance as their neighbours. In addition, there is the possibility that unresolved astronomical waves, forced to have the same admittance as their neighbours in a group under the constant admittance assumption, are modelled poorly and can therefore modulate one of the principal constituents.

of the results must take this into account, since the importance of interaction of the Hanning data window with the synthesised data depends on the position of the filled gap within the sample epoch. Figure 4 shows the relative weighting of data by the Hanning window as a function of position in the data window. Data near the ends contribute little to the analysis results when weighted by the Hanning window. The relative contribution of the synthesized data, in terms of its weighting, to the analysis of each overlapping sample epoch has been computed on this basis and each one classified according to whether the contribution is less than 10%, between 10% and 20% or greater than 20%. We consider that estimates affected at a level greater than 20% are not reliable. Although this treatment is not an ideal solution, it goes further than most in dealing with the difficult problem of data continuity, and represents an attempt to get the most out of what amounts to an average working data set. More recent data have fewer gaps and their analysis will not be contaminated to the same degree.

A representative estimate of the mean tidal admittance is necessary for comparison of the average coherency among the three borehole tiltmeters and the vault measurements, and to compare the observations with the theoretical tilt based on a marine loading model (section 4). Schuller [1977] argues that the best, unbiased estimate of the mean admittance is derived from the means of the in-phase and quadrature components of the time varying admittance function determined as above, since any bias due to aliasing is avoided. The error in the estimate is derived from the variance of the time varying admittance function.

equi-spaced time series and care must be taken to avoid aliasing. The Nyquist frequency is given by $\omega_v = \pi/\Delta T$, where ΔT is the time shift of the sequential epochs. The maximum frequency present in the admittance function is determined by the bandwidth of the Hanning window, $B_h = 4\pi/T$, where T is the length of the sample epoch. Thus the condition, $\Delta T < T/4$, determines the minimum time shift required to avoid aliasing in the sequential analysis. The sample epoch for the present analysis was chosen to be 1440 hours in order to separate the main tidal constituents, and the time shift set to 288 hours, which satisfies the above condition. However, the amplitude of the first side-lobe of the Hanning window is 2.6% of that of the main lobe, which therefore potentially allows some leakage between waves separated by frequencies in the range of 138.89 uHz ($4\pi/T$) to 208.33 uHz ($6\pi/T$). Among the major constituents, only N_2 will be affected by significant leakage (from M_2) so that the N_2 admittance function should be interpreted carefully on account of small but possibly significant aliasing effects.

Apart from the fact that a continuous record is desirable if we hope to reliably detect departures from a stable admittance function, it is also logistically necessary if we wish to perform the type of analysis described above. Inevitably, gaps exist in our data and, after filtering, with attendant loss of data, amount to approximately 18% for 106 and 12% for 107 of the total recording period. Gaps can be interpolated within the HYCON procedure using the synthesised tide based on the mean admittance of the total data set. Any interpretation

spectral side-lobes associated with the rectangular window have an effect even in regression analysis. We are penalised in this, however, because the Hanning spectral window broadens the spectral peaks by comparison with those given by the equivalent rectangular data window. Therefore the minimum data window must be increased to two months in order to avoid the leakage of energy between major constituents, especially M_2 and N_2. This increase correspondingly reduces the number of independent estimates of the admittance for the second and longer data set to six.

Our approach to the analysis of potentially non-stationary tidal signals is to assume that admittance changes are sufficiently slow that two month samples may be considered to be stationary. By analysing samples that overlap in time we expect to detect variations in the Earth's tidal response, or the tidal forcing, as changes in the average admittance from one sample to the next. In practice, the sequence of average admittances (which we will refer to as the admittance function) may reflect apparent, but unreal time variations which result from either the inaccuracy of the assumption that the admittance is constant within a wave group, or from the effects of non-linear or other waves of a non-astronomical origin that are not included in the analysis. In both cases periodicities will be induced which result in a time varying admittance function due to intermodulation. Considerable care is required to properly detect such modulation and to distinguish it from real time variations in the earth response or the tidal forcing.

As pointed out by Schuller [1977], the admittance functions are

variations in the constituents where it is necessary to avoid the confusion between actual changes in the earth response or the tidal forcing, and apparent admittance changes due to modulation when finite samples of the data are analysed. We have used the HYCON method of Schuller [1977] in which the original 505 astronomical waves have been reduced to 73 whose theoretical earth tide amplitudes (ignoring tidal loading) are greater than 0.1 nrad. This represents a compromise between the cost of computation and the precision required of the analysis. It will be shown later that the background noise is sufficiently high that the effects of omitted astronomical waves are not significant. Since waves closely spaced in frequency cannot be resolved for the data window used, waves clustered around each of the 10 main constituents are grouped and each group is assumed to have a constant admittance.

The HYCON procedure involves the computation of the theoretical earth tide, and the setting up and solution of the least squares normal equations in terms of the admittance of the observed data to the body tide input. The associated error for the estimates is computed for each tidal band (diurnal, semi-diurnal and ter-diurnal) on the basis of the frequency dependant residual variance determined from the Fourier analysis of the residual time series [Schuller, 1977].

One of the chief advantages of the HYCON method is that it combines the spectral analysis technique of windowing the data, using the Hanning window, with the least squares analysis for the admittance of the tidal groups. The approach recognises that the effects of the

For calibration cycles in which the background noise was normal, the standard deviations were typically at the level of the resolution of the digitising table (0.1mm or 0.5nrad). Figure 3 shows the calibration amplitudes recorded on the primary recorders for tiltmeters 106 and 107. The scale factor for each channel is determined to better than 0.1%.

Prior to analysis the data were digitally filtered to separate the tides from the long period and secular components of the signal. For the harmonic analysis a 61 point symmetrical bandpass filter designed to reject the diurnal and semi-diurnal bands was used. The response of the filter was computed for each tidal frequency in the harmonic analysis and the computed amplitudes corrected for the small effects, typically 0.1%, of the filtering. A low pass filter was used to prewhiten the data prior to the power and high resolution spectral analyses and the estimates were subsequently corrected for its effect.

3.2 Harmonic Analysis

The aim of harmonic analysis of the tilt data is to determine accurately the amplitudes and phases of constituents of known frequency within the data. For this study the constituents of interest are those tidal constituents of astronomical origin which contain sufficient energy either to be recognisable above the noise, or those that are unresolved in the analysis yet must be included in the solution to avoid significant modulation of the adjacent waves in the spectrum. The latter consideration is particularly important in the study of time

instruments, but essential for the study of time variations in tidal admittance from which the effects of sensitivity changes of the tiltmeter and the recording system must be eliminated.

3. DATA ANALYSIS

3.1 Data Preparation

The data analysed in this study were recorded during the periods 27/Sept/80 to 29/June/81 (tiltmeter 105 in borehole 1) and 27/Nov/81 to 31/Dec/82 (tiltmeters 106 and 107 in boreholes 2 and 1, respectively). All data were recorded on strip chart recorders at a recording speed of 30mm per hour and at a sensitvity of approximately 0.2 mm per nrad. Hourly time marks were superimposed on the recordings and the data digitised at these marks. Spurious points, resets and short thermal trends were removed and a few gaps of under 24 hours duration were manually interpolated on the basis of data before and after the gap. This was possible because the long period trends in the data change slowly in comparison with the tide.

The data were scaled using calibration factors derived from twice weekly in situ calibration sequences. The mean and standard deviation of each sequence was computed and, since most changes in the calibration amplitudes corresponded with recorder changes, a scale factor was determined for each recorder channel using the weighted mean of the calibration amplitudes determined from data registered on that channel.

lack of it, in the tidal constituents. By "true" variability we mean fluctuations that require an interpretation in terms of time changes in the Earth's response to the tidal forcing, or changes in the tidal forcing itself. Our aim is first to eliminate apparent variations which are either artifacts of the analysis procedure, or are due to intermodulation between constituents not separable over the analysis epoch. An examination of the physical causes of the variability that we establish will be the subject of a separate study.

The results of the overlapping two-monthly HYCON analyses described in section 3.2 are plotted in figures 13 to 18. The amplitude and phase estimates for tiltmeter 105 operating in borehole 1 for M_2, N_2, S_2K_2, O_1 and $P_1S_1K_1$ are plotted against the central time of the data window in figures 13 and 14. The relative influence of interpolated gaps (see section 3.2) is indicated at the top of each figure for each sample series by symbols explained in the caption for figure 13. The significance of admittance variations plotted in the panels below should be judged in the light of these qualitative confidence estimates because the effects of a poor interpolation model cannot be distinguished from an admittance variation. Less weight should be given to estimates from series for which the interpolation effect is greater than 20% than those where the corresponding effect is less than 10%.

In general, the variability of the estimates for tiltmeter 105 is within or close to the 95% confidence envelope (shown by the dotted curves in the plots), indicating that from a statistical point of view with respect to the residual noise, the variations are hardly signific-

ant. Despite this, there does seem to be an underlying correlation between the admittance curves in the two component directions for each wave. The M_2 south and east amplitudes both show a broad peak spanning the winter months (December to March) while the phase lags are reasonably stable. The south and east N_2 estimates exhibit troughs both in amplitude and phase lag during the winter, while S_2 trends steadily to increasing amplitude and phase lag through most of the 9 month period. Although the diurnal constituents are not as well determined, the amplitude and phase lag variations of $P_1S_1K_1$ and O_1, respectively, are quite similar in both azimuths.

It is apparent from these data that the range of the amplitude variations is much the same for all of the constituents (between 2 and 6 nrad). Thus, the fractional amplitude changes in M_2 amount to about 6% and for the diurnals, up to 50%. We will look now at the results from the second data set (tiltmeters 106 and 107, figures 15 to 18) to see if the behaviour noted for 105 persists beyond the first period in borehole 1, and if that behaviour is coherent between the two boreholes.

Although the gaps in the observed 106 and 107 data are in most cases quite short (2 to 4 days) and the number of gaps small (7 for 106 and 8 for 107) their effect has propogated widely through the sequential analyses. The distribution of gaps is quite different for the two installations, but nearly the same for both components of the same tiltmeter. Out of 29 points, only 12 are affected at less than 10% for each instrument, 26 at less than 20% for 107 and 15 under 20% for 106.

The plots therefore have to be interpreted carefully. Ignoring the gap problem for the moment, we will look at the general behaviour of the data and subsequently determine if the features remain under closer scrutiny.

In a similar way to 105 operating in borehole 1 the variations in the four components are, in most cases, hardly significant in terms of the 95% confidence error envelope. Nevertheless, among the semi-diurnal waves there are particularly strong correlations between the admittance curves from the orthogonal components of the same instruments. With the exception of N_2 in the south, we can also detect a clear but somewhat weaker correlation between the estimates determined in the same azimuth from the two instruments. So it appears, for the semi-diurnals at least, that there is better agreement between the south and east estimates in a given borehole than between redundant measurements made in the two boreholes. This is disturbing because it suggests that a measurement effect is influencing the estimates. The patterns of the diurnal admittance variations (figures 17 and 18) are, on the other hand, quite distinct in either direction and correlate well between the boreholes.

There are two other general features of the data that are consistent with the 105 data set. Firstly, the absolute range of the variations is similar for the five constituents irrespective of wave amplitude. Secondly, there is no discernible correlation between the variations of the different waves. Thus, we cannot identify a systematic semi-diurnal or diurnal characteristic behaviour.

If we examine the semi-diurnal admittance variations in conjunction with the interpolation distribution, it becomes clear that for the "reliable" data (the subset of the overlapping analysis results in which points contaminated by interpolation at a level greater than 20% are ignored), there is a strong correlation both between orthogonal directions of the same instrument and from one instrument (or borehole) to another. Moreover, the lack of correlation between components from the two boreholes can be explained by the difference in interpolation effects. We can expect that if the south and east components of the measurement are really varying in the same way, then the admittance curves will be distorted in the same way by the same distribution of interpolated data. Such an effect would leave the orthogonal components of each of the tiltmeters highly correlated, as observed. Since the gaps in the two tiltmeter records occur at different times, distortions in the admittance curves will arise at different times and the maximum differences will occur where the interpolation effect is large for one data set and small for the other. The major contrasts occur at analyses 1, 9, 22, 23, 27 and 28. Eliminating 22 and 23 of 107 M_2 makes all four components agree in both amplitude and phase lag. An improvement is made for N_2 by disregarding analyses 9, 22 and 23, although the south direction variations remain poorly correlated between the instruments. In the case of S_2, for which the inter-instrument correlations are good, little improvement is gained by considering interpolation effects.

The diurnal results are quite well correlated between instruments,

yet the style of the variations is different in the two azimuths. In most cases, particularly in the south components, the variability is greatest during the winter months at the same time that the least squares errors are largest.

5.5 Polar plots of the variability of the M_2 and O_1 admittances.

The results shown in figures 15 to 18 can also be presented as polar plots in which variations in admittance trace out a path, with a surrounding swath of error estimates, in polar coordinates. Figures 19 and 20 show these phasor trajectory plots of M_2 and O_1 for 106 and 107 south and east components. The points are plotted using symbols, as described earlier, indicating the effect of interpolation. Ninety-five per cent error circles have been plotted for each point and then, to avoid confusion, largely erased leaving only a representative arc labelled by the analysis number. The reader can reconstruct the complete plot from the information shown.

Following the procedure used earlier to represent the weighting of the data points according to the symbols, we have attempted to identify the most likely paths of the admittance variations. The interpretation is shown in figure 21 which should be considered in conjunction with figures 19 and 20. Looking at M_2 first, the resemblance between the two east components is remarkable and is firmly based on the "under 10%" interpolation effect data. Even the early data (analyses 1 to 5), where 106 suffers from large interpolation errors, correlate closely in their behaviour. The strong trend from analyses 6

to 15 occurs during the spring and comprises a combined amplitude decrease of about 5% and phase lag increase of 2.5 to 3 degrees. From mid-June to mid-August (analyses 15 to 20) only the amplitude changes, increasing by 3.5% in 106 and 4.5% in 107. This is followed by a period of greater stability in analyses 21 to 25 which are well determined, and in 26 to 29 which are less well determined in tiltmeter 106.

In the south direction, the resemblance between the two M_2 trajectories is less impressive. However an early, predominantly phase, trend (analyses 1 to 5) and its well determined reversal during the spring (6 to 15), show the same level of variation as in the east direction. The fluctuations after this time are relatively small and are not well correlated between the instruments. Certainly, the period covered by analyses 21 to 29 is obviously one of greater stability for both components and it is probable that statistical uncertainties in the analysis results obscure any correlation between trajectory paths.

The O_1 trajectories are more complex. In the east direction, most of the variations are in phase lag during the first four and last three months of the series. In between, the admittance is fairly stable. The behaviour of the 107 south trajectory is similar to those of the east direction except that the variations are in amplitude rather than phase lag. The trajectory of 106 south appears to undergo two anti-clockwise rotations about the mean until it reverts to a cyclical amplitude variation similar to 107 south.

While these interpretations cannot be regarded as definitive, they

represent in our estimation the most obvious trends in the time variation of the admittances. It is important to note that by comparison with the confidence estimates, only the maximum excursions are even marginally significant at the 95% level and that with only one instrument we would have difficulty in producing convincing arguments for variability. The close correlation between the two instruments suggests that our error estimates, based on noise estimates over a whole frequency band, are overly pessimistic. The importance of observations from two or more instruments is again confirmed.

We must now investigate whether the variability that we have described above is real, or an artifact of the analysis procedure.

5.6 High resolution Fourier analysis of the residuals.

The interaction between the Hanning window and gaps in the data has already been discussed and its effect minimised. The main concern now is the effects of any systematic modulation from waves, within 0.39 μHz (tidal analysis bandwidth) around the major constituents, that were ignored or poorly modelled in the harmonic analysis.

The diurnal and semi-diurnal portions of the high resolution Fourier spectrum of the residuals (section 3.3) for both components of tiltmeters 106 and 107 are plotted in figures 22 and 23 with a linear amplitude scale. The "background" noise in the diurnal band for all four components is essentially flat with an approximate level of 1 nrad. In the semi-diurnal band, however, the residual noise rises, for

each component, from a backround of 0.3 nrad to a broad peak spanning the interval 21 to 23 μHz with a particular concentration of energy, in the south components, around $2N_2$. The broad feature resembles the "cusp" commonly observed in marine tides [Munk et al, 1965] and tilt and strain observations affected by marine tidal loading (for example, Peters [1978]; Beavan and Goulty [1977]). It is attributed (Munk et al, [1965] to non-linear interactions between the strong tidal constituents and the low frequency continuum, and shallow water non-linear interactions among the tidal constituents themselves. The cusp rises to a level around 0.75 nrad in the east and 1 nrad in the south and is consistent with the M_2 constituent RMS errors derived from the sequential harmonic analyses (figure 24). At this point we see the justification for choosing a subset of the original 505 astronomical waves for the HYCON analysis. We chose a cutoff for the body tide amplitude of 0.1 nrad (leaving 73 waves in the analysis) and few, if any, of the neglected waves appear to be significant in the residual spectrum. These constituents are sufficiently below the observed background noise to make inter-constituent modulation insignificant, even for a signal augmented by marine loading. The effect of the general background noise level has already been included in the error analysis for the two monthly data sets.

A closer inspection of the semi-diurnal spectrum shows holes in the vicinity of the main tidal lines which results from the least squares removal of energy at those frequencies. Rising significantly above the background in all four components, but most pronounced in

106, is a pair of peaks located at a distance of one resolution bandwidth either side of M_2. This is the spectral representation of the observed, "around 6 month" cycle identified in the M_2 admittance variations. That this is an isolated and significant pair indicates that the variation is real and not due to intermodulation effects. No such behaviour is apparent for N_2, or S_2 which showed a less significant variation in amplitude. The residual spectra of both azimuths of 107 have a potentially significant line near 22 μHz which may introduce a degree of modulation. The source of the 60 to 80 day periodicity noted in N_2 is not clear, although, given the high residual amplitude levels near the N_2 frequency, some modulation may be expected.

The two prominent peaks in the south direction (near 21.5 μHz) coincide with the $2N_2$ and μ_2 constituents which are included in the linear harmonic analysis. Godin [1973], in his analysis of marine tides at Québec, has, however, identified μ_2 as a double constituent, sharing its frequency with the non-linear interaction $2M_2-S_2$. He has also detected the nonlinear wave O_2 between $2N_2$ and μ_2. A similar effect may occur in the loading near the Charlevoix site. If this is so, the non-linear part will remain because the $2N_2$ group cannot be realistically modelled with a constant admittance.

6. DISCUSSION

Spatial coherency of tilt observations is essential if they are to be interpreted in terms of regional crustal properties and processes.

The general lack of spatial coherency among measurements within a region (or even beside one another) is related to the ubiquitous presence of meteorological noise, and the departure on all length scales of the crust from lateral homogeneity. The advent of borehole and long baseline measurements has increased the potential for achieving interpretable results. However, most of the traditional objectives of earth tide research - refining global Love numbers, discriminating between crustal models and solving the inverse marine loading problem - require, as Baker [1979] points out, regionally representative tidal response estimates accurate to better than 2-5%. It is considered unlikely that locally generated tilt perturbations and associated model corrections will, in general, be reduced to those levels. Our experience at Charlevoix provides a dramatic demonstration of the problem. The borehole installations were designed with a view to minimising the sensitivity of the measurements to local strain-tilt coupling effects. Yet the mean M_2 tidal amplitudes differ by 20% between borehole 1 and borehole 2 with no observable discontinuity present in the terrain. Effects of this magnitude are rare but disturbing and serve to emphasise the difficulties associated with determining absolute response estimates with any confidence.

Recent crustal deformation research using the earth tide has focused on the investigation of large-scale crustal discontinuities such as batholiths and thrust faults [Edge et al, 1983; Bonatz et al, 1983]. So long as a reasonable degree of spatial coherency can be established, the large (up to 50%) anomalies generated by lateral

elastic property contrasts may be able to provide constraints on the structure of these features that are complementary to seismic studies [Harrison, 1976].

In studies of time variations in the tidal admittance we are no longer shackled to the need for a structurally interpretable measurement. There remains, however, the need for spatial coherency of the relative changes in admittance over length scales smaller than the prospective active area. It is therefore essential, as in all regional studies using point observations, that redundant measurements be made. We have observed remarkable agreement between the time varying admittances determined in two boreholes, lending credence to a regional interpretation. Nevertheless, the study of relative changes in the tidal parameters introduces a new set of interpretation problems and ambiguities.

There are few acknowledgements in published studies of time varying tidal admittance of the inherent difficulties in fitting a stationary, deterministic regression model to a finite length, gappy representation of a non-stationary, partly deterministic collection of processes. Schuller [1977] has made an important contribution to the treatment of this problem, allowing for a "piecewise stationary" model and using the Hanning data window to avoid modulation due to spectral leakage. Complications arising from the interaction of interpolated gaps with the data window have been addressed in the present study as well as the importance of verifying the absence of intermodulation through detailed examination of the mean admittance residual spectrum.

Interpretation of the determined semi-diurnal and diurnal admittance variations at Charlevoix is in progress. Since the major component of the signal at the Charlevoix site arises from loading by the St. Lawrence River tide, we expect that variations in the load will be reflected in the tilt. Indeed, as noted in section 5, the observed tilt admittance variations neither indicate consistent fractional changes in amplitude, nor characteristic diurnal or semi-diurnal patterns, both features that are expected to accompany changes in crustal response. Preliminary estimates of the M_2 admittance variations from the tide gauge at St. Joseph de la Rive immediately south of the site correlate reasonably well with the tilt results. Thus it is clear that a detailed evaluation of the stability of the input must be made before conclusions can be reached about possible changes in crustal response.

The prominent features in the borehole secular tilt correlate with the transient and seasonal behaviour of the water table. Although the tilt series are not long enough to indicate established long term trends, we can get an idea of the lower limit of the detectability of regional signals from the difference in the long term drift rates between the redundant 106 and 107 measurements. A crude estimate, based on the 5 months of data following the reinstallation in July, 1982 of tiltmeter 106, is 2 μrad/yr in the south direction and 0.4 μrad/yr in the east. The difference between these rates points to possible problems with reference point stability. By comparison, Buchbinder et al [in press] conclude that, after the reduction of

groundwater effects in the 40m baseline levelling array at the Charlevoix site, the uncertainty with which tectonic tilts could be detected falls within a range of 4-6 μrad. In terms of drift rate, their data suggest that a persistent trend over a year or more of 4 μrad/yr would be detectable. This is considerably worse than the borehole results and arises from the dominance of groundwater (and probably thermal) effects which are at least 5 times larger than in the boreholes. During the comparative tilt experiment at Piñon Flat, Wyatt et al [1982] measured long term drift rates of approximately 4 μrad/yr in the 26m borehole and 0.7 μrad/yr using the surface 535m baseline fluid tiltmeter. These results suggest that the baseline of a surface tiltmeter needs to be an order of magnitude greater than the borehole depth to achieve comparable performance.

7. CONCLUSIONS

An array of three borehole tiltmeters has been established at Charlevoix Observatory, Québec to study the tidal and secular response of the crust within the Charlevoix seismic zone. Differences in the M_2 tidal results as large as 20% in amplitude and 5 degrees in phase were found between two boreholes 80m apart. Theoretical M_2 amplitudes and phases computed from the tidal loading model of the St. Lawrence River were systematically different from all of the observed results, indicating that unconsidered local topographic and geological strain-tilt coupling effects, in addition to regional structural features are to

some extent distorting the response. The O_1 mean admittances were consistent among the different observations and in good agreement with theory.

Time variations in the tidal admittance were observed for the major constituents M_2, N_2, S_2K_2, O_1 and $P_1S_1K_1$. Although the variations were not in general statistically significant at the 95% level (based on the least squares residual variance) they were remarkably consistent between the two boreholes, indicating that errors based on the residual variance tend to overestimate the uncertainty of the admittance determination. It is believed that fluctuations in the load tide are at least partly responsible for the observed behaviour. However, it is important to note that the physical significance of the variations would have remained undetected if there had been measurements only from a single borehole. Once again the importance of redundant measurements is confirmed.

The borehole secular tilt is correlated with water table fluctuations, the typical coefficient being approximately 0.5 μrad/m. A preliminary estimate of the lower detectable limit of long term regional anomalies, using simultaneous measurements from two boreholes, is 0.4 μrad/yr - comparable with the lowest rates so far reported.

The Charlevoix Region

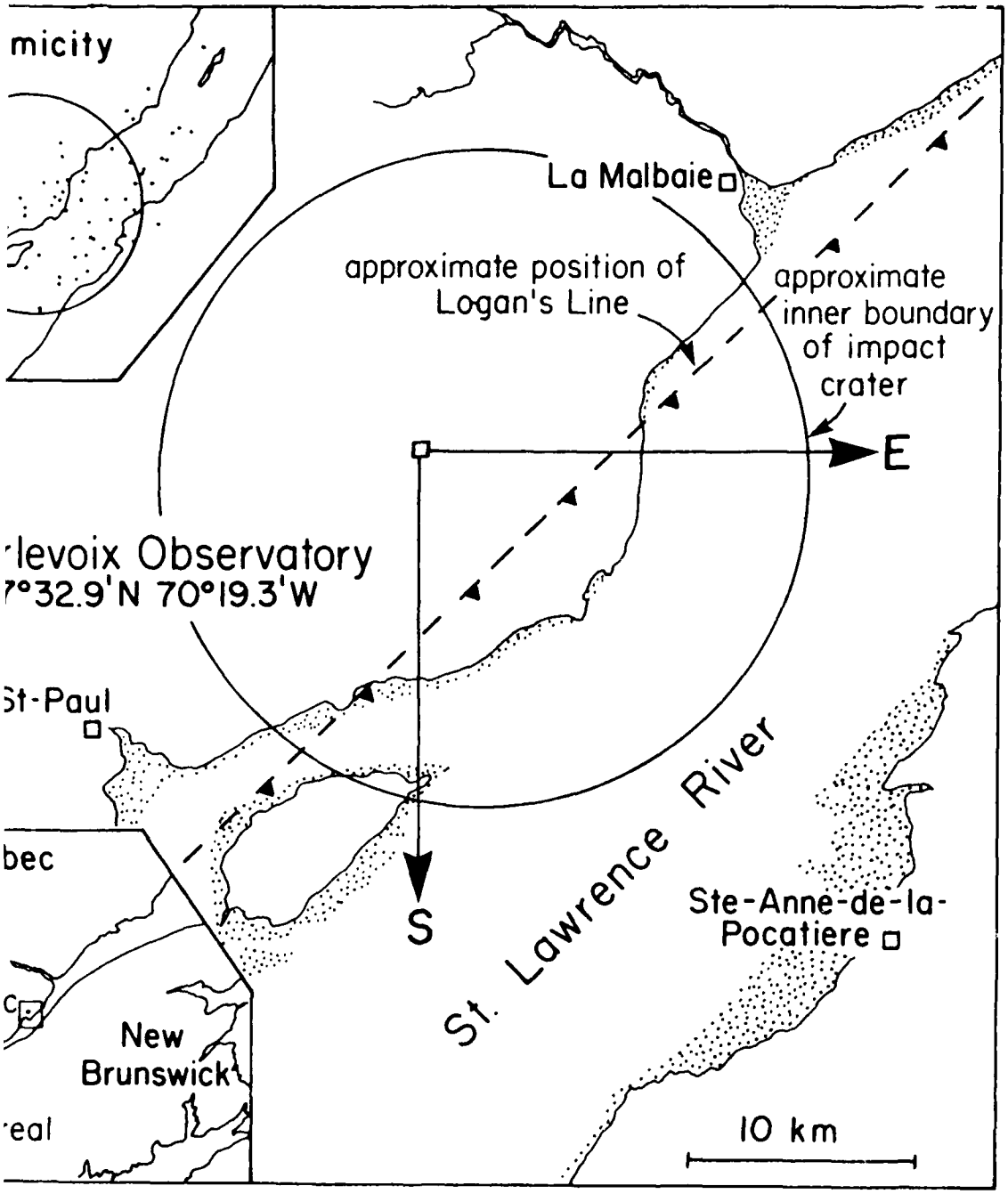

Figure 1

Figure 23. Semi-diurnal band high resolution Fourier amplitude residual spectra of the 106 and 107 south and east components. Details as described in figure 22.

Figure 24. Plots versus time of the 106 and 107 south and east RMS amplitude errors associated with M_2 amplitude estimates from the HYCON sequential analysis.

lags for O_1 and $P_1S_1K_1$. Details as described for figure 13.

Figure 19. Polar trajectory plots of the 106 and 107 south and east M_2 admittances estimated from the HYCON sequential analysis. The observed mean admittance vector is shown in the upper part of each diagram. The shape surrounding the end point of the vector corresponds with the dashed curve surrounding the detailed trajectory plot. Each point on the trajectory is represented by a symbol indicating the degree to which that estimate is influenced by interpolated gaps (see text). Filled circles indicate an influence less than 10%, squares less than 20% and triangles greater than 20%. Points associated with triangles are least reliable. Part of the 95% error circle associated with each estimate is indicated by a matching sequence number in sloping numerals.

Figure 20. Polar trajectory plots of the 106 and 107 south and east O_1 admittances estimated from the HYCON sequential analysis. Details as described in figure 19.

Figure 21. Polar trajectory interpretation. Qualitative representation of the admittance time variations shown in figures 19 and 20.

Figure 22. Diurnal band high resolution Fourier amplitude residual spectra of the 106 and 107 south and east components, based on the mean tidal admittance determined from the HYCON sequential analysis. Spectral estimates are plotted at approximately half the resolution bandwidth of 58.5nHz.

Figure 13. Plots versus time of the south and east tidal amplitudes for M_2, N_2, S_2, O_1 and $P_1S_1K_1$ estimated from the HYCON sequential analysis of tiltmeter 105 data from borehole 1. The solid curves join points representing the amplitudes while the dotted curves indicate the 95% error envelopes. The points are positioned in time at the middle of each analysis epoch. Symbols at the top of the diagram indicate the degree to which the individual estimates are influenced by interpolated gaps (see text). Filled circles indicate an influence less than 10%, squares between 10% and 20% and triangles greater than 20%. Points associated with triangles are least reliable.

Figure 14. Plots versus time of the south and east Greenwich phase lags for M_2,N_2,S_2,O_1 and $P_1S_1K_1$ estimated from the HYCON sequential analysis of tiltmeter 105 data from borehole 1. Details as described for figure 13.

Figure 15. Plots versus time of the south and east tidal amplitudes for M_2,N_2 and S_2 estimated from the HYCON sequential analysis of tiltmeters 106 and 107 data from simultaneous operation in boreholes 2 and 1, respectively. Details as described for figure 13.

Figure 16. Plots versus time of the 106 and 107 south and east Greenwich phase lags for M_2,N_2 and S_2. Details as described for figure 13.

Figure 17. Plots versus time of the 106 and 107 south and east tidal amplitudes for O_1 and $P_1S_1K_1$. Details as described for figure 13.

Figure 18. Plots versus time of the 106 and 107 south and east Greenwich phase

arrows. The error bars represent 95% confidence bounds on the randomness of the background noise. Logarithms are to base 10.

Figure 11. Comparison plot of tilt and strain background noise spectra taken from various sites:- Piñon Flat, California: laser strainmeter [Berger and Levine, 1974], fluid tiltmeter [Wyatt et al, 1982]; Queensbury, U.K.: laser strainmeter [Beavan and Goulty, 1977]; Poorman mine, Colorado: laser strainmeter [Berger and Levine, 1974], Hughes bubble tiltmeter [Harrison, 1976]; Llanrwst, U.K.. fluid tiltmeter [Peters, 1978]; Charlevoix, Québec: borehole tiltmeter (present study). The sampled points are represented by filled circles in the case of strain and filled triangles for the tilt measurements. Logarithms are to base 10.

Figure 12. Polar diagrams showing the comparison with theory of the mean M_2 and O_1 admittances observed for the south and east components of tiltmeters 105 (borehole 1), 106 (borehole 2), 107 (borehole 1) and the ANAC tiltmeters operating in the observatory vault. G is the Greenwich phase lag. The ANAC results are taken from Peters et al, [1983] and rotated into their south and east components by combining the redundant A and C measurements with the single orthogonal D measurement. The theory is represented in the upper part of each diagram by the sum of the body tide (vector 1), the far-field load (vector 2) and the local load (vectors 3 and 4; see text). The lower part of the diagrams shows the detailed comparison between the observations and theory. The circles represent 95% errors on the mean admittance estimates.

the Charlevoix site shown below it in detail. It is the loading from the estuary that contributes the local or '3' and '4' components of the tilt phasors in figure 12.

Figure 6. Empirical M_2 cotidal chart for the St. Lawrence estuary, with detail of the area adjacent to the Charlevoix site. Dots represent the location of tide gauge installations.

Figure 7. Empirical O_1 cotidal chart for the St. Lawrence estuary, with detail of the area adjacent to the Charlevoix site. Dots represent the location of tide gauge installations.

Figure 8. Plots versus time of secular tilt for a) tiltmeter 105 operating in borehole 1 from Sept. 1980 to June, 1981; b) tiltmeters 106 and 107 operating in boreholes 2 and 1, respectively, from Nov., 1981 to Dec., 1982. Also shown for both periods are manual measurements of water level taken from well B(70).

Figure 9. Secular tilt trajectories of tiltmeter 105 operating in borehole 1 and tiltmeters 106 and 107 operating in boreholes 2 and 1 for the same periods indicated in figure 8. Each trajectory describes the path taken by the bottom of the freely hanging pendulum relative to the instrument body. Reference times are marked by full circles and show the Julian day number and year.

Figure 10. Residual power spectra of the south and east components of tiltmeters 106 and 107 operating in boreholes 2 and 1, respectively. The observed M_2 and O_1 power levels are indicated by the tip of the

FIGURE CAPTIONS

Figure 1. Location of the Charlevoix Observatory. The lower inset shows the observatory area in relation to the St. Lawrence Valley. The upper inset shows the spatial relationship of seismicity in the region to the zone of deformation associated with the Charlevoix crater (after Lyons et al [1980]).

Figure 2. Upper part. Plan view of the Charlevoix Observatory showing the locations of the three boreholes; water wells A(70 m deep), B(two wells 30 m and 70 m deep) and C(134 m deep); the tilt and strain observatory vault; and the 40 m baseline levelling array. Lower part. Cross-sectional view of the borehole layout.

Figure 3. Plot versus time of calibration amplitudes for recorder channels monitoring tiltmeter components 106X, 106Y, 107X and 107Y. Each amplitude determination is represented by a vertical bar the mid-point of which is the amplitude, and the length equal to twice the 95% error. The amplitudes are normalized by the weighted mean of each sequence.

Figure 4. Estimating the weighting of a data subset as a function of its position within the Hanning data window. For example, a data subset spanning the interval from 0.8T to 0.9T will contribute 4.1% of the total weight.

Figure 5. Triangular division, for the load calculations, of the whole of the St. Lawrence River estuary (upper diagram) with the area adjacent to

Sbar, M.L., and R.L. Sykes, Contemporary compressive stress and seismicity in Eastern North America: An example of intra-plate tectonics. Geol.Soc. Am.Bull., 84, 1861-1881, 1973.

Schuller, K., Tidal analysis by the Hybrid Least Squares Frequency Domain Convolution Method, in: Proceedings of the Eighth Int. Symp. on Earth Tides, M. Bonatz and P. Melchior eds., Institut fur Theoretische Geodesie Der Univ. Bonn, Fed. Rep. Germany, 1977

Tanaka, T., Effect of Dilatancy on Ocean Load Tides, Pageoph., 114, 415-423, 1976.

Wyatt, F., G. Cabaniss and D.C. Agnew, A comparison of tiltmeters at tidal frequencies, Geophys. Res. Letters, 9, 743-746, 1982.

Zschau, J., Tidal sea load tilt of the crust, and its application to the study of crustal and upper mantle structures, Geophys. J. R. astr. Soc., 44, 577-593, 1976.

Milne, W.G., W.E.T. Smith, and G.C. Rogers, Canadian seismicity and microearthquake research in Canada, Can. J. Earth Sci., 7, 591-601, 1970.

Mortenson, C.E. and M.J.S. Johnston, The nature of surface tilts along 85 Km of the San Andreas Fault - preliminary results from a 14 instrument array, Pageoph, 113, 237, 1975.

Munk, W.H., B. Zetler, and G.W. Groves, Tidal Cusps, Geophys. J. R. astr. Soc., 10, 211-219, 1965.

Nishimura, E., On Earth Tides, Trans. A.G.U., 31, 357-375, 1950.

Peters, J.A., The construction of a cased borehole facility for the purpose of tilt observations at Charlevoix Observatory, Québec, Earth Physics Branch open file report no. 83-21, 1983.

Peters, J.A., Tidal measurements using a new long baselength tiltmeter, unpub. Ph.D. thesis, Univ. of Liverpool, England, 1978.

Peters, J.A., D.R. Bower, and A. Lambert, Tidal tilt response at Charlevoix, Québec, in: Proceedings of the Ninth Int. Symp. on Earth Tides, J.T. Kuo ed., E. Schweizerbart'sche Verlagsbuchhandlung, 1983.

Robertson, P.B., Zones of shock metamorphism at the Charlevoix impact structure, Québec, Geol. Soc. Am. Bull., 86, 1630-1638, 1975.

Robertson, P.B., La Malbaie structure, Québec - a Paleozoic meteorite impact site. Meteoritics, 4, 89-112, 1968.

That of the Tides, Ph.D. thesis, Technichen Universitat Clausthal, 1976, AFGL-TR-77-0162 (Translation), 1979.

Kato, M., Observations of Crustal Movements by Newly-Designed Horizontal Pendulum and Water-Tube Tiltmeters with Electromagnetic Transducers (2), Bull. Disast. Prev. Res. Inst. Kyoto Univ., 29, Part 2, 83-97, 1979.

Leblanc, G., and G. Buchbinder, Second microearthquake survey of the St. Lawrence Valley near La Malbaie, Québec, Can. J. Earth Sci., 14, 2278-2789, 1977.

Leblanc, G., A.E. Stevens, R.J. Wetmiller, and R. DuBerger, A microearthquake survey of the St. Lawrence valley near La Malbaie, Québec, Can. J. Earth Sci., 10, 42-53, 1973.

Lyons, J.A., D.A. Forsyth, and J.A. Mair, Crustal studies in the La Malbaie region, Québec, Can. J. Earth Sci., 17, 478-490, 1980.

McConnell, R.K., Jr. and J. Lewkowicz, Research on the nature of ground tilts in the period range 10^3 to 10^7 seconds, AFGL-TR-78-0105, Weston Observatory, Boston College, 1978.

Mikumo,T., M.Kato, H.Doi, Y.Wada, T.Tanaka, R.Shichi, and A. Yamamoto, Possibility of temporal variations in earth tidal strain amplitudes associated with major earthquakes, in: Earthquake Precursors, Kisslinger, C. and Suzuki, Z., eds., Can. Acad. Publ. Japan, Tokyo, 1978.

Lake District, in: Proceedings of the Int. Workshop on Monitoring Crustal Dynamics in Earthquake Zones, F. Vieweg and Sohn Verlag, 1979.

El-Sabh, M.I., T.S. Murty et L. Levesque, Mouvements des eaux indiuts par la marée et le vent dans l'estuaire du Saint-Laurent, Le Naturaliste Canadien, 106, 89-104, 1979.

Flach, D., W. Grosse-Brauckmann, K. Herbst, G. Jentzsch and O. Rosenbach, Results of long-term recordings with Askania borehole tiltmeters - Comparative Analysis with respect to the tide parameters and long period portions and instrumental investigations, Deutsch. Geodat. Komm, B211, 72-95, 1975.

Flach, D. and O. Rosenbach, The Askania borehole tiltmeter (tide pendulum) of A. Graf at the Zellerfeld - Muhlenhohe testing station, Bull. Inf. Mar. Terr., 60, 2934-2943, 1971.

Godin, G., Eight Years of Observations on the Water Level at Québec and Grondines 1962-1969, Manuscript Report Series 31, Marine Sciences Directorate, Dept. Environment, Canada, 1973.

Harrison, J.C., Tilt observations in the Poorman mine near Boulder, Colorado, J. Geophys. Res., 81, 329, 1976a.

Harrison, J.C., Cavity and Topographic Effects in Tilt and Strain Measurement, J. Geophys. Res., 81, 319, 1976b.

Herbst, K., Interpretation of Tilt Measurements in the Period Range Above

293-305, 1977.

Berger, J., and J. Levine, The spectrum of earth strain from 10^{-8}Hz to 10^{2}Hz, J. Geophys. Res., 79, 1210-1214, 1974.

Bonatz, M., C. Gerstenecker, R. Kistermann, and J. Zschau, Tilt measurements across a deep fault zone, Proceedings of the Ninth Int. Symp. on Earth Tides, J.T. Kuo ed., E. Schweizerbart'sche Verlagsbuchhandlung, 1983.

Bower, D.R., The Measurement of the Earth Tide and Regional Heterogeneity Due to the Ocean Tide, unpub. Ph.D. thesis, Univ. of Durham, England, 1971.

Buchbinder, G., R. Kurtz, and A. Lambert, A review of time-dependent geophysical parameters in the Charlevoix Region, Québec, Earthquake Prediction Research, in press.

Cabannis, G.H., The measurement of long period and secular deformation with deep borehole tiltmeters, in: Applications of Geodesy to Geodynamics, I. Mueller ed., Ohio State University Press, 165-169, 1978.

Edge, R.J., T.F. Baker, and G. Jeffries, Some Results from Simultaneously Recording Tiltmeters, Proceedings of the Ninth Int. Symp. on Earth Tides, J.T. Kuo ed., E. Schweizerbart'sche Verlagsbuchhandlung, 1983.

Edge, R.J., T.F. Baker, and G. Jeffries, Earth Tides: Tilt in the English

REFERENCES

Agnew, D.C., Nonlinearity in rock: evidence from earth tides, J. Geophys. Res., 86, 3969-39, 1981.

Agnew, D.C., Strain tides at Piñon Flat: Analysis and interpretation, unpub. Ph.D. thesis, Univ. of California, San Diego, 1979.

Beaumont, C., Linear and nonlinear interactions between the earth tide and a tectonically stressed earth, in: Applications of Geodesy to Geodynamics, I. Mueller, ed., Ohio State University Press, 313-318, 1978a.

Beaumont, C., Tidal loading: crustal structure of Nova Scotia and the M_2 tide in the northwest Atlantic from tilt and gravity observations, Geophys. J. R. astr. Soc., 53, 27-53, 1978b.

Beaumont, C., and R. Boutilier, Tidal loading in Nova Scotia: results from improved ocean tide models, Can. J. Earth Sci., 15, 981-993, 1978.

Beaumont, C., and J. Berger, Earthquake prediction: modification of the earth tide tilts and strains by dilatancy, Geophys. J. R. astr. Soc., 39, 111-121, 1974.

Beaumont, C., and A. Lambert, Crustal structure from surface load tilts, using a finite element model, Geophys. J. R. astr. Soc., 29, 203-226, 1972.

Beavan, R.J., and N.R.Goulty, Earth-strain observations made with the Cambridge laser strainmeter, Geophys. J. R. astr. Soc., 48,

ACKNOWLEDGEMENTS

This project was supported by the Air Force Geophysics Laboratory, Hanscom AFB (under contracts F19628-80-C-0032 and F19628-83-K-0023), the Natural Sciences and Engineering Research Council through Operating and Equipment grants and the Gravity, Geothermics and Geodynamics Division of the Earth Physics Branch. We would like to thank Ross Boutilier who performed the loading calculations and provided invaluable computing and field assistance. We are grateful to Gerry Cabannis, Tony Lambert and Don Bower for their interest and support throughout the program and to Jacques Labrecque for his assistance in operations at the Charlevoix Observatory. Benoit Dostaler and Josee Laurion maintained the array on a day to day basis and Jim Covill assisted with data reduction and analysis. Terry Collins skillfully drafted the diagrams.

Charlevoix Observatory, Québec

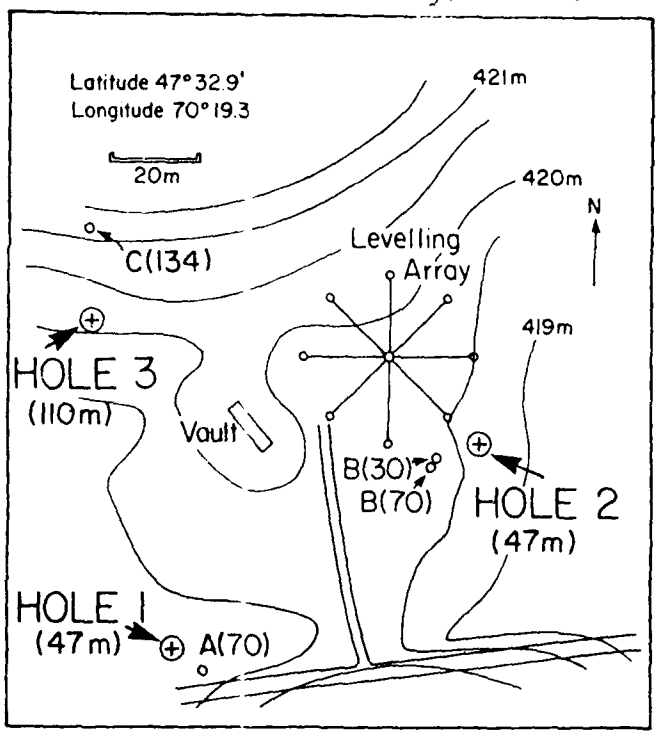

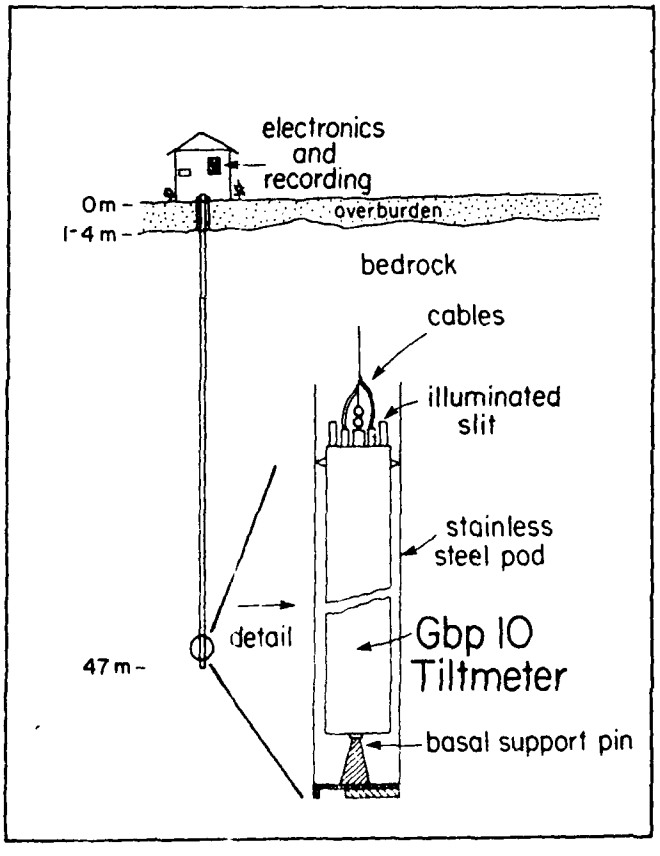

Figure 2

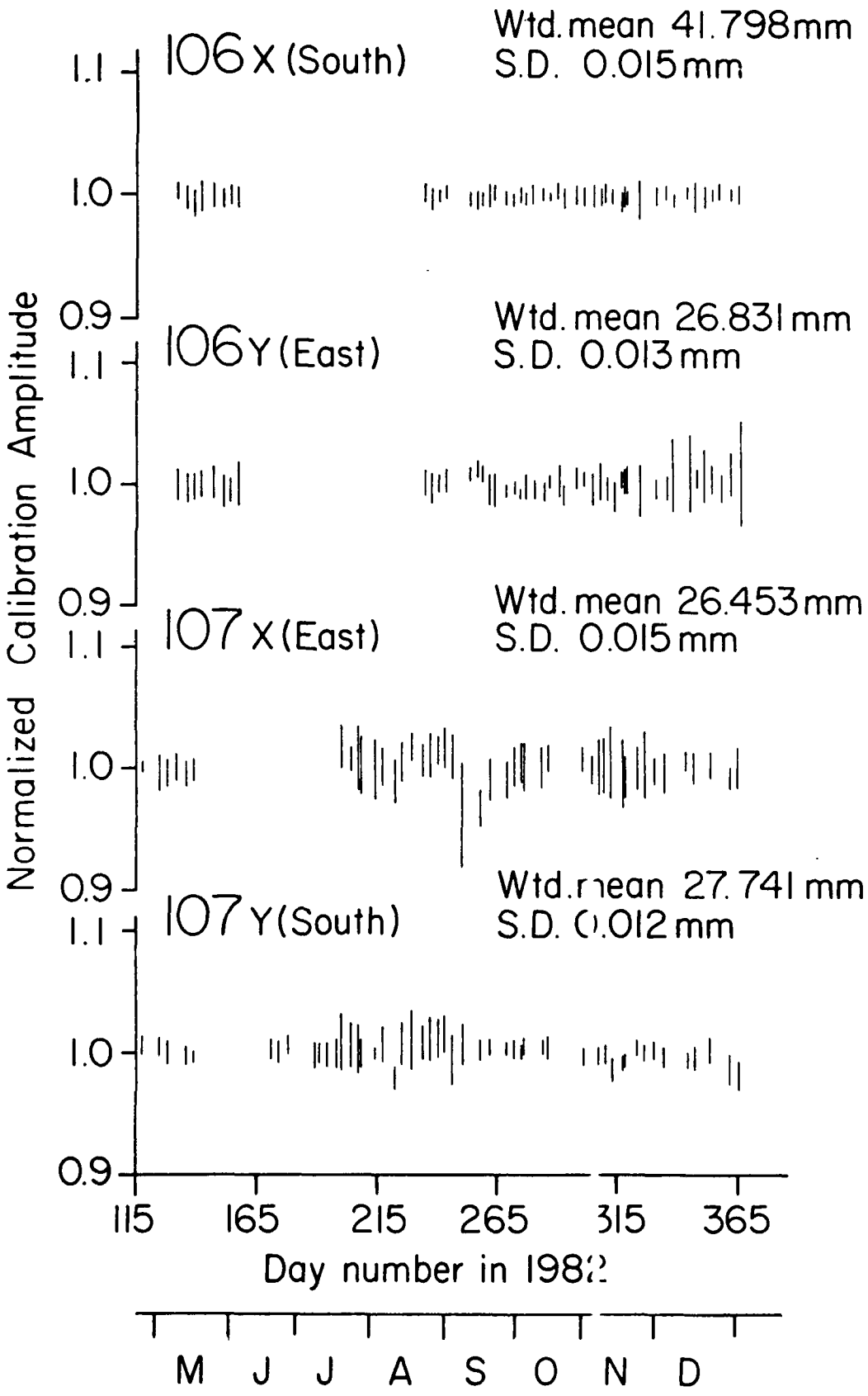
Wtd. mean 41.798mm
S.D. 0.015mm
106X (South)
Wtd. mean 26.831mm
S.D. 0.013mm
106Y (East)
Wtd. mean 26.453mm
S.D. 0.015mm
107X (East)
Wtd. mean 27.741mm
S.D. 0.012mm
107Y (South)
Normalized Calibration Amplitude
1.1
1.0
0.9
115
165
215
265
315
365
Day number in 1982
M J J A S O N D

Figure 3

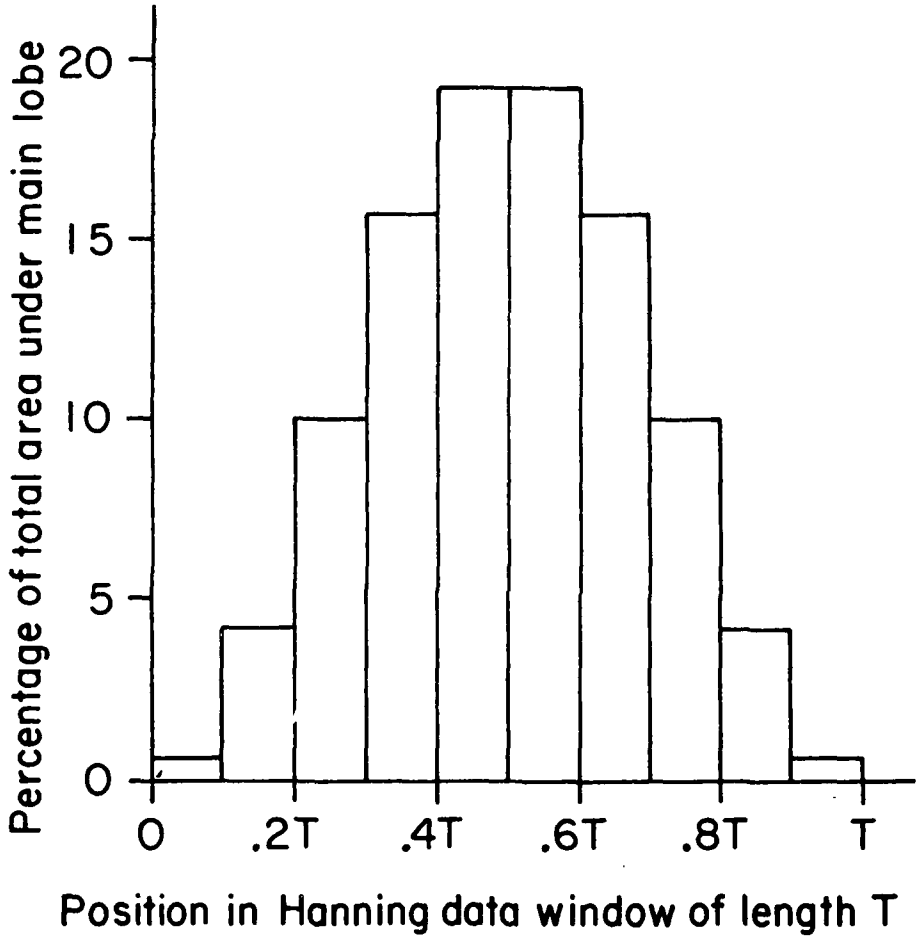
Percentage of total area under main lobe
20
15
10
5
0
0
.2T
.4T
.6T
.8T
T
Position in Hanning data window of length T

Figure 4

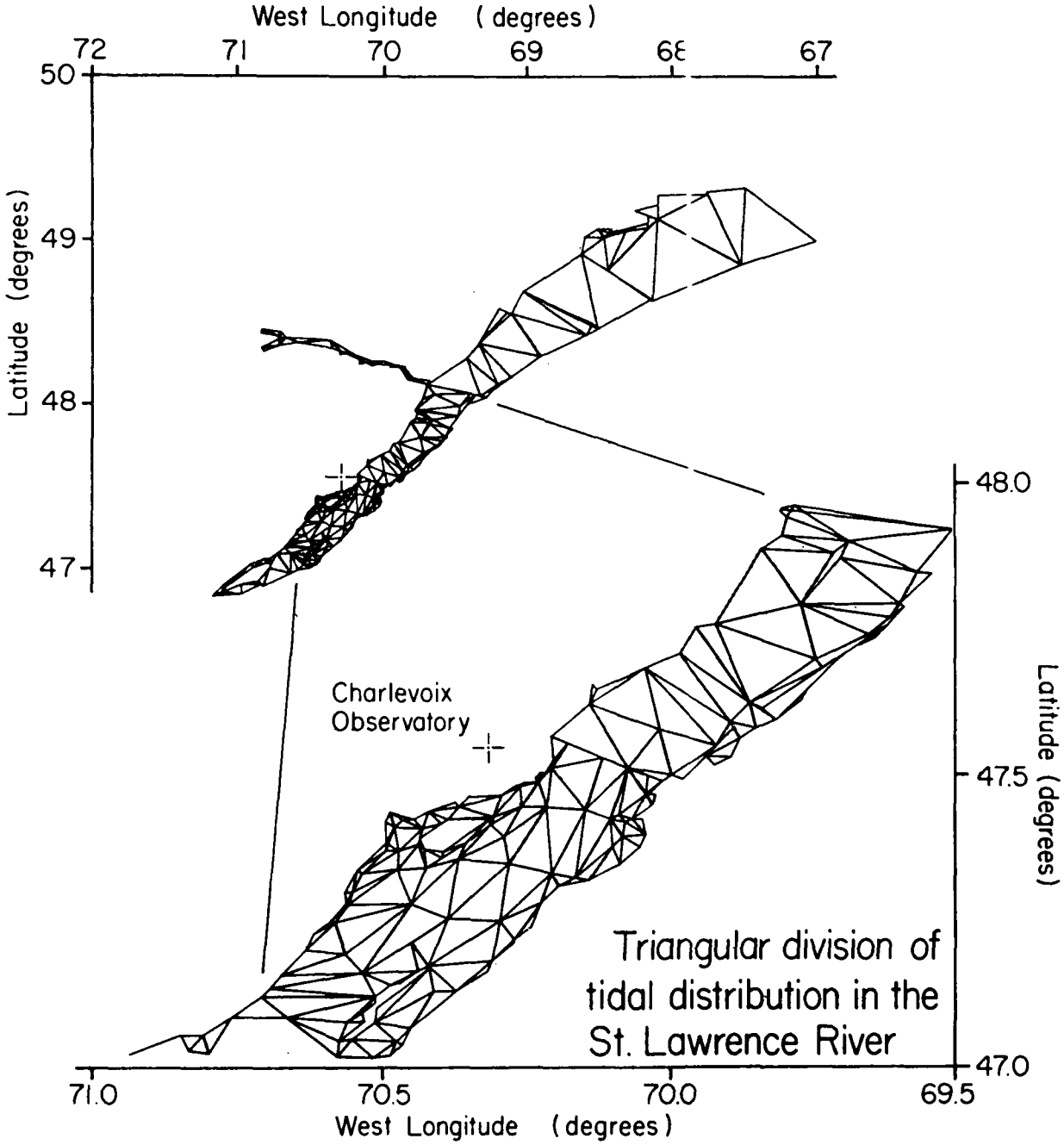
West Longitude (degrees)
72
71
70
69
68
67
50
49
48
47
Latitude (degrees)
Charlevoix
Observatory
48.0
47.5
47.0
Latitude (degrees)
Triangular division of
tidal distribution in the
St. Lawrence River
71.0
70.5
70.0
69.5
West Longitude (degrees)

Figure 5

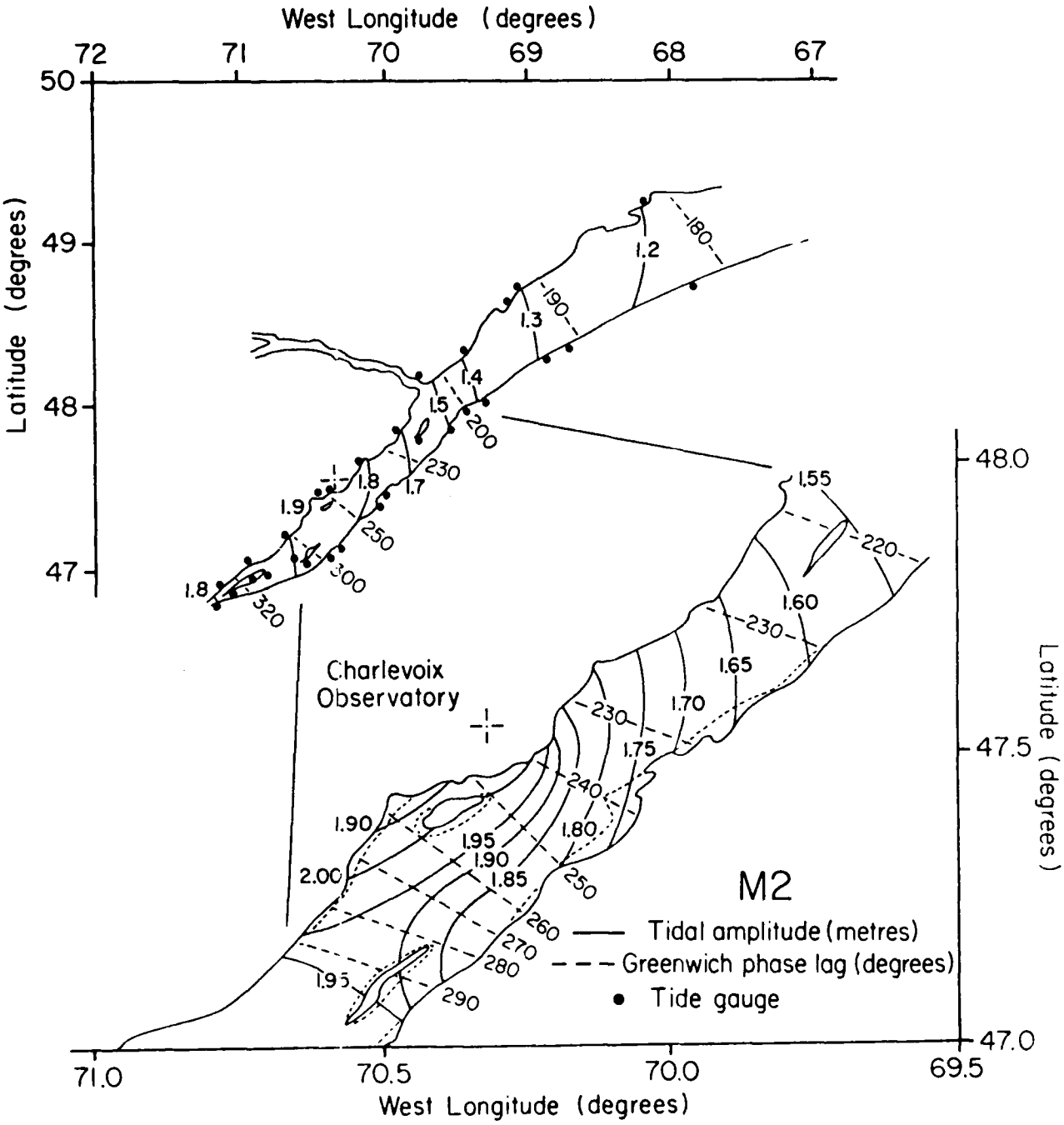
West Longitude (degrees)
72
71
70
69
68
67
50
49
48
47
Latitude (degrees)
1.2
180
190
1.3
1.4
1.5
200
230
1.8
1.7
1.9
250
300
1.8
320
1.55
220
1.60
230
1.65
1.70
230
1.75
240
1.80
1.90
1.95
1.90
1.85
2.00
250
260
270
280
290
1.95
Charlevoix
Observatory
M2
Tidal amplitude (metres)
Greenwich phase lag (degrees)
Tide gauge
48.0
47.5
47.0
Latitude (degrees)
71.0
70.5
70.0
69.5
West Longitude (degrees)

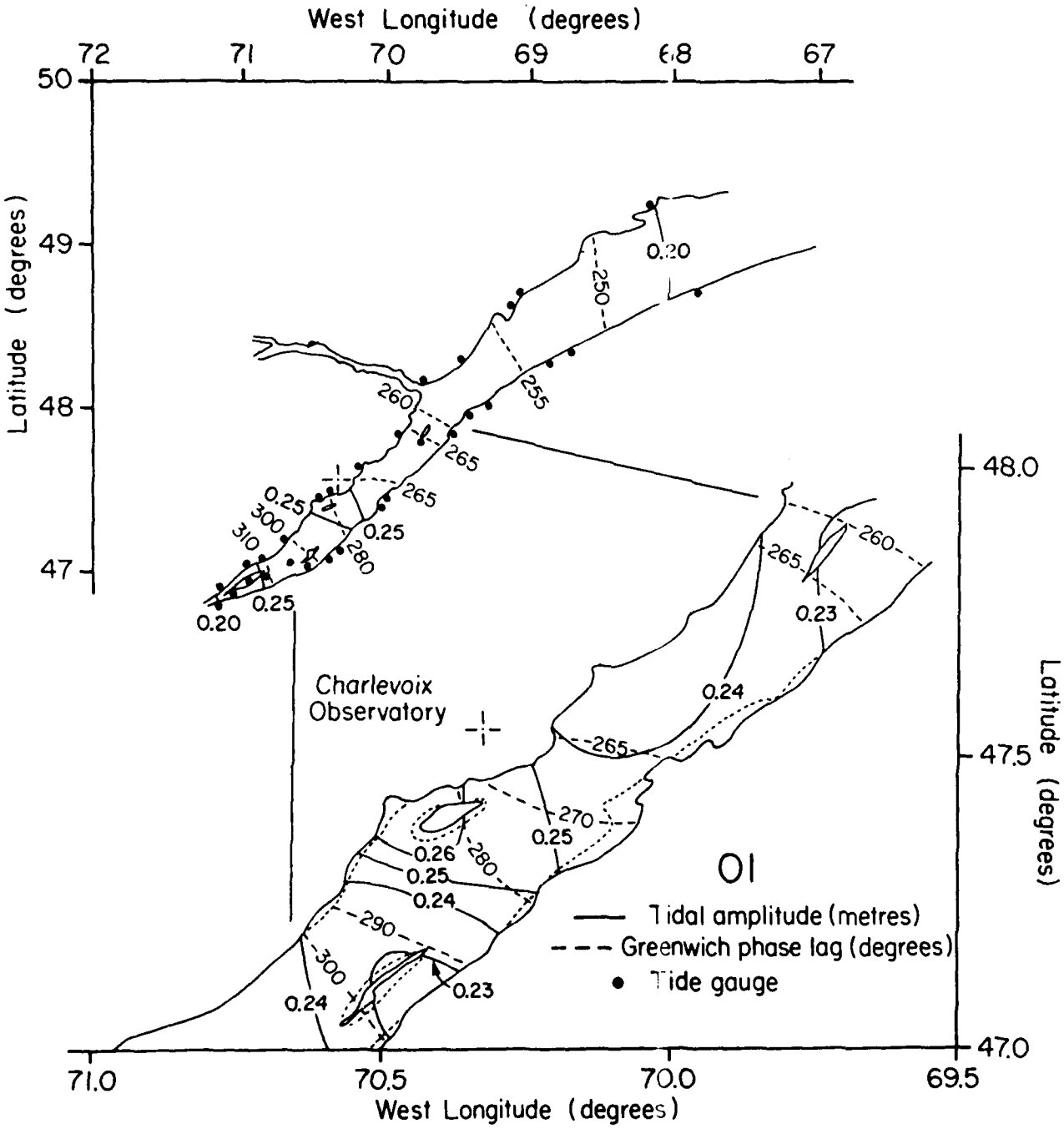
West Longitude (degrees)
72
71
70
69
68
67
50
49
48
47
Latitude (degrees)
0.20
250
255
260
265
0.25
300
310
280
Charlevoix
Observatory
48.0
47.5
47.0
Latitude (degrees)
0.23
0.24
270
0.26
290
01
Tidal amplitude (metres)
Greenwich phase lag (degrees)
Tide gauge
71.0
70.5
70.0
69.5
West Longitude (degrees)

Figure 7

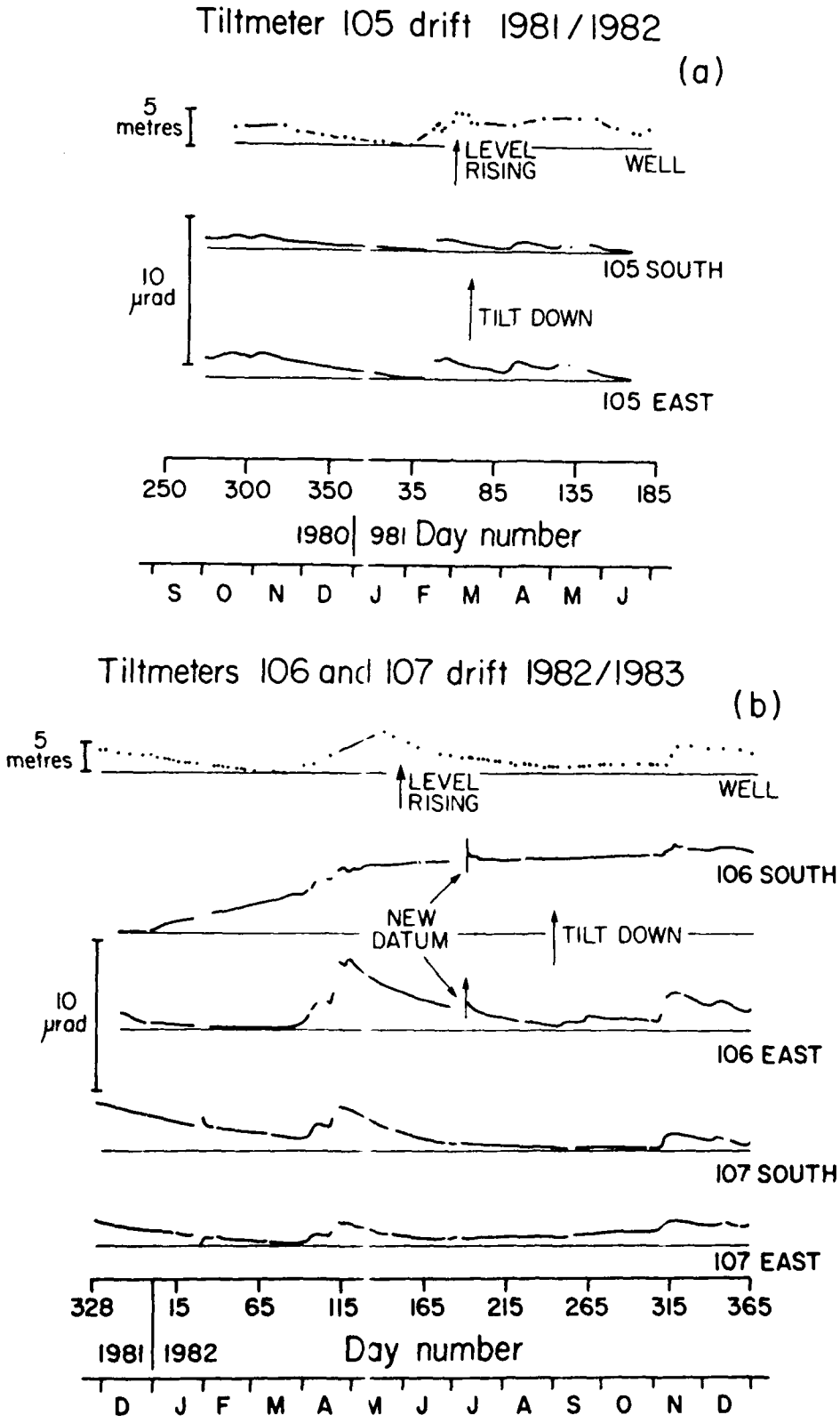
Tiltmeter 105 drift 1981/1982
(a)
5 metres
LEVEL RISING
WELL
10 μrad
105 SOUTH
TILT DOWN
105 EAST
250 300 350 35 85 135 185
1980 981 Day number
S O N D J F M A M J
Tiltmeters 106 and 107 drift 1982/1983
(b)
5 metres
LEVEL RISING
WELL
106 SOUTH
NEW DATUM
TILT DOWN
10 μrad
106 EAST
107 SOUTH
107 EAST
328 15 65 115 165 215 265 315 365
1981 1982 Day number
D J F M A M J J A S O N D

Figure 8

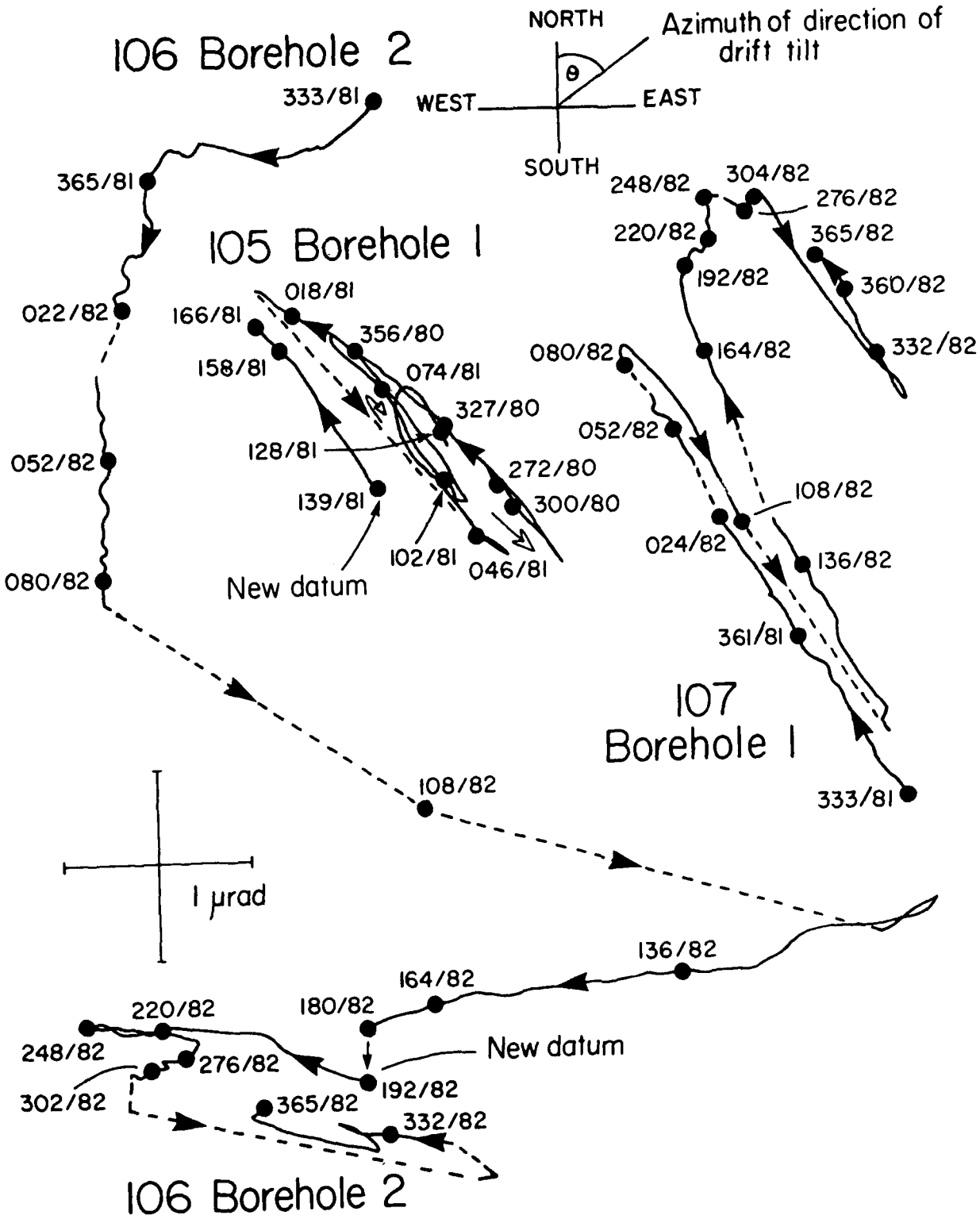
NORTH
Azimuth of direction of drift tilt
θ
WEST
EAST
SOUTH
106 Borehole 2
333/81
365/81
022/82
052/82
080/82
105 Borehole 1
018/81
166/81
356/80
158/81
074/81
327/80
128/81
272/80
139/81
300/80
102/81
046/81
New datum
248/82
304/82
276/82
220/82
365/82
192/82
360/82
164/82
332/82
080/82
052/82
108/82
024/82
136/82
361/81
107
Borehole 1
333/81
108/82
1 μrad
136/82
164/82
180/82
220/82
New datum
248/82
276/82
192/82
302/82
365/82
332/82
106 Borehole 2

Figure 9

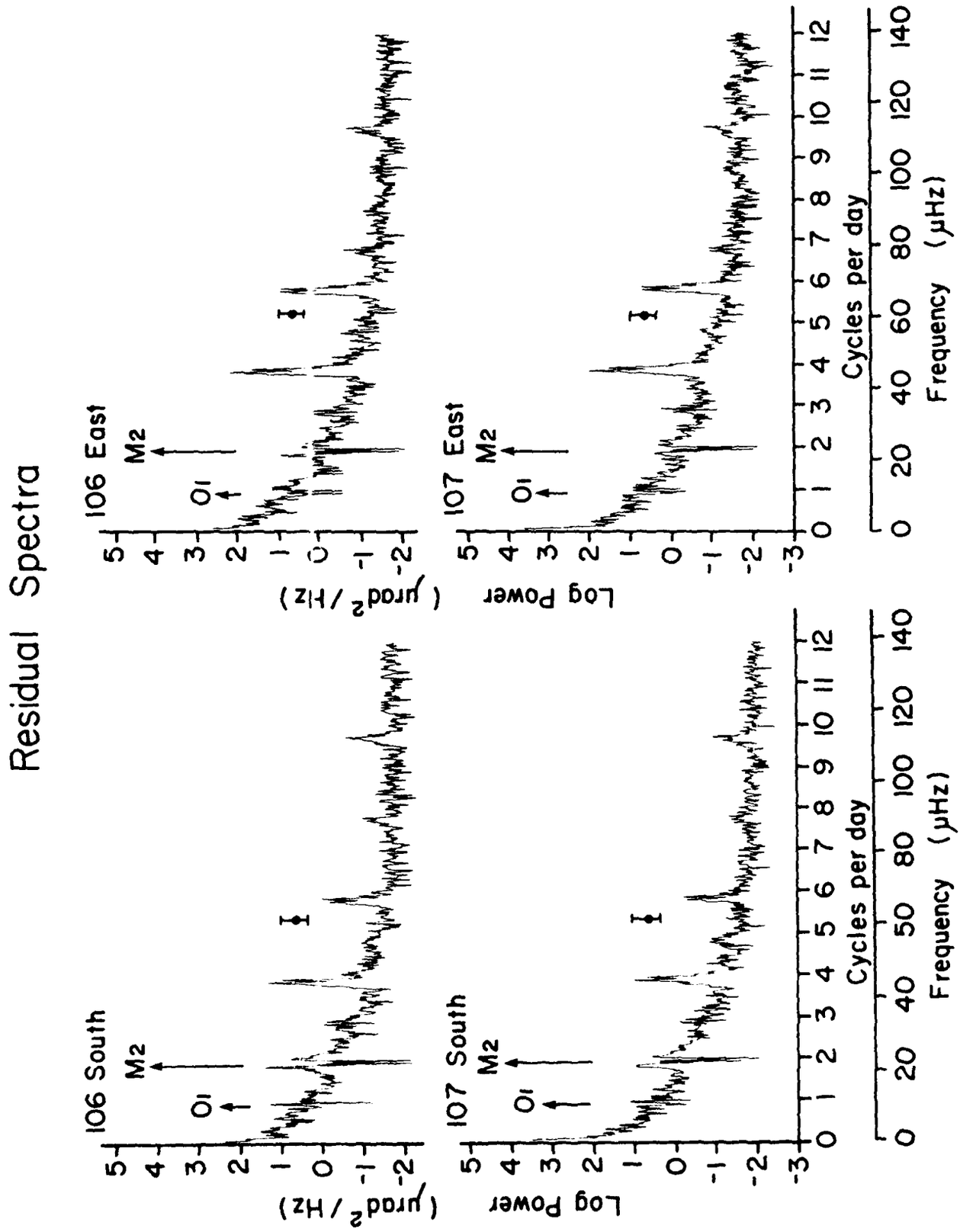
Residual Spectra
106 South
106 East
107 South
107 East
M2
O1
(μrad²/Hz)
Log Power
Cycles per day
Frequency (μHz)

Figure 10

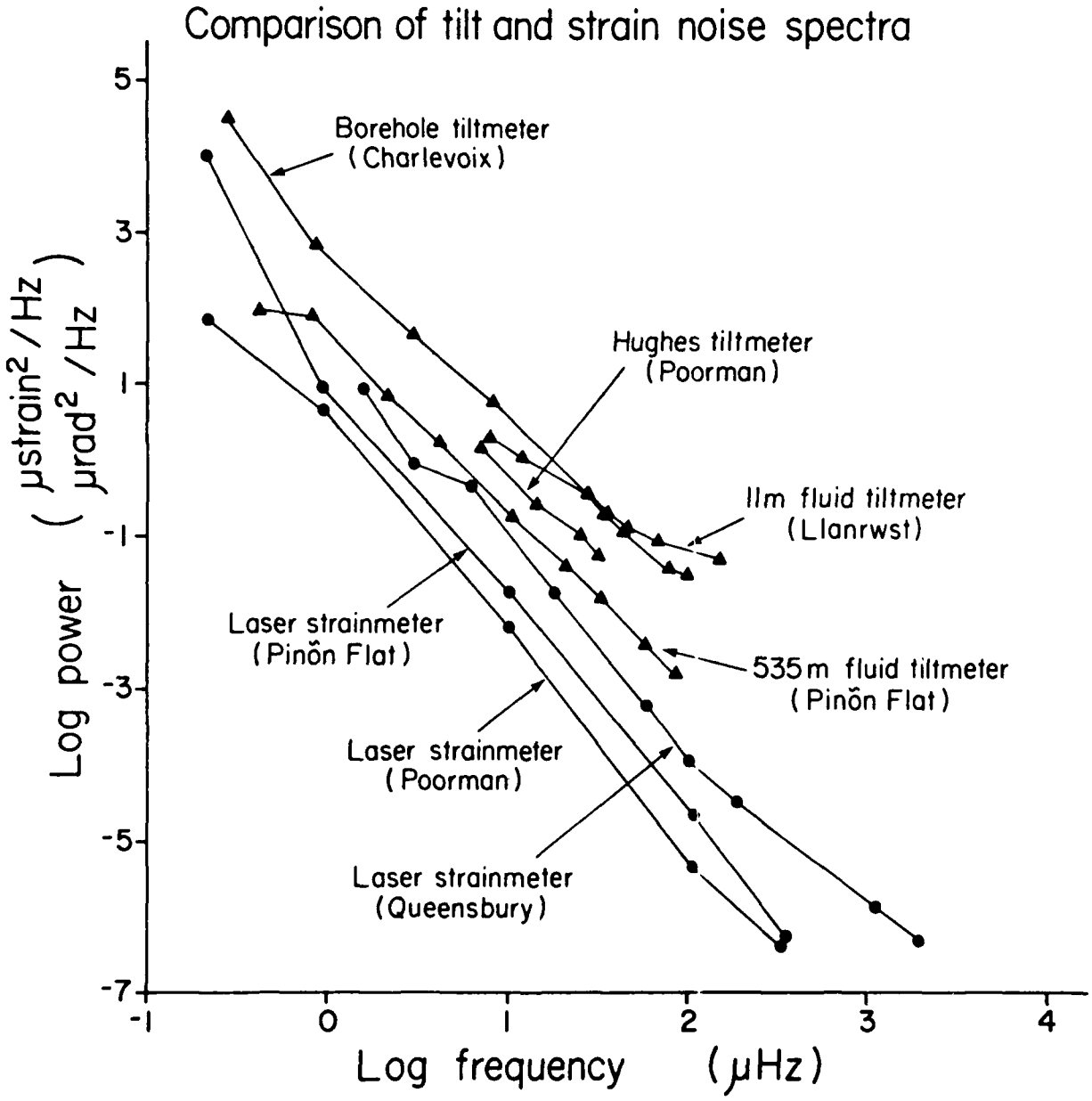
Comparison of tilt and strain noise spectra
Borehole tiltmeter
(Charlevoix)
Hughes tiltmeter
(Poorman)
11m fluid tiltmeter
(Llanrwst)
Laser strainmeter
(Pinõn Flat)
535m fluid tiltmeter
(Pinõn Flat)
Laser strainmeter
(Poorman)
Laser strainmeter
(Queensbury)
Log power (μstrain²/Hz / μrad²/Hz)
Log frequency (μHz)
5
3
1
-1
-3
-5
-7
-1
0
1
2
3
4

Figure 11

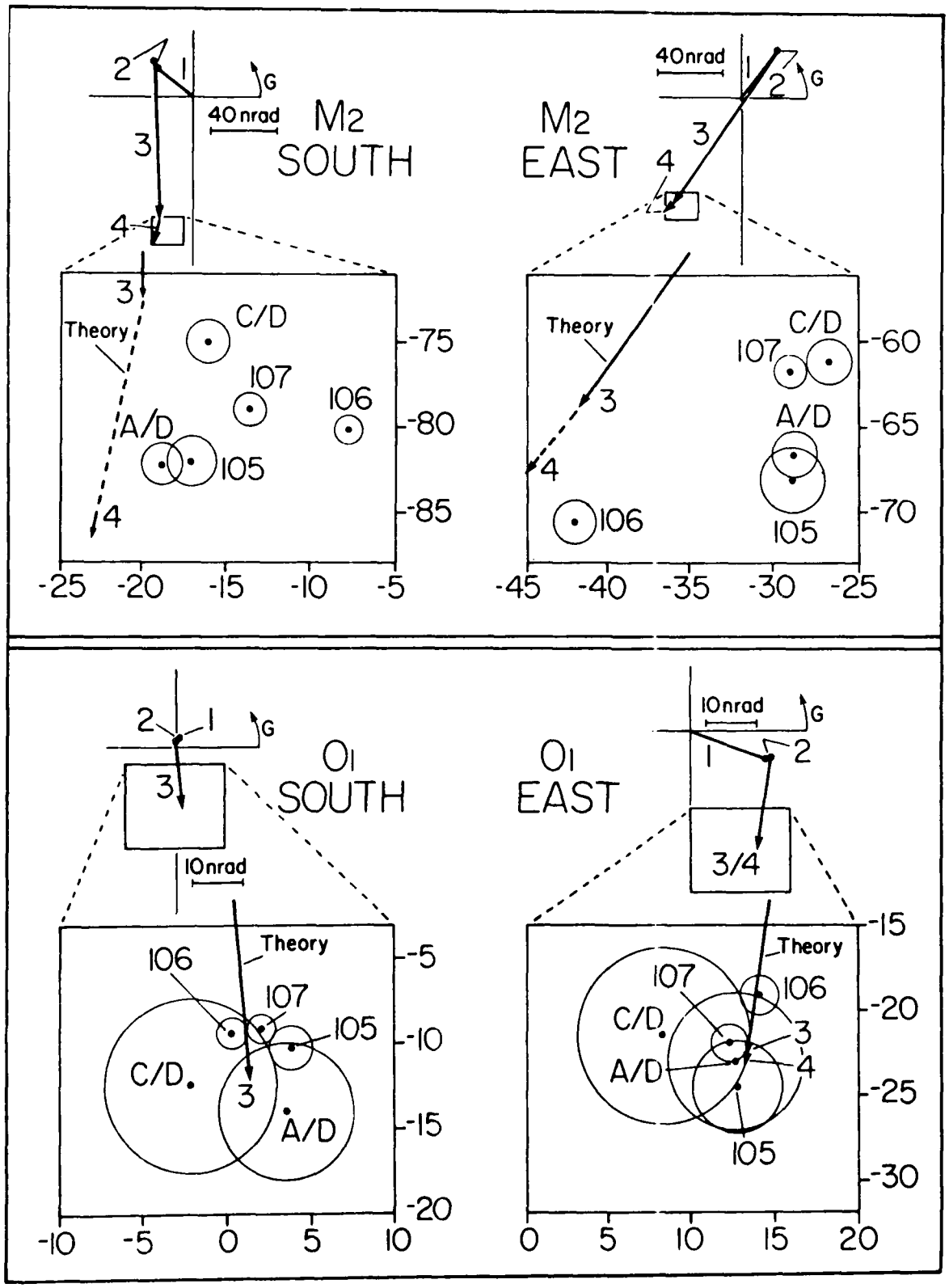
M2
SOUTH
40nrad
G
Theory
C/D
107
106
A/D
105
-75
-80
-85
-25
-20
-15
-10
-5
M2
EAST
40nrad
G
Theory
C/D
107
A/D
105
106
-60
-65
-70
-45
-40
-35
-30
-25
O1
SOUTH
10nrad
G
Theory
106
107
105
C/D
A/D
-5
-10
-15
-20
-10
-5
0
5
10
O1
EAST
10nrad
G
Theory
107
106
C/D
A/D
105
3/4
-15
-20
-25
-30
0
5
10
15
20

Figure 12

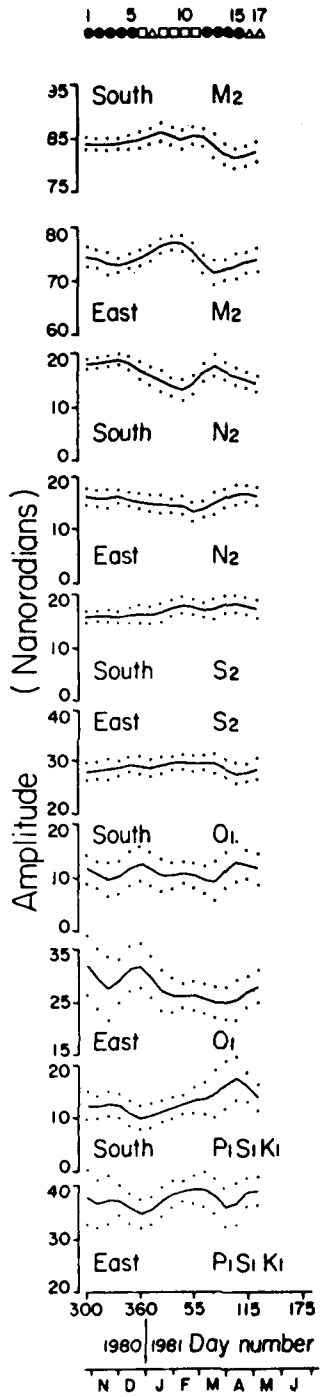
1 5 10 15 17
South M2
East M2
South N2
East N2
South S2
East S2
South O1
East O1
South P1 S1 K1
East P1 S1 K1
Amplitude (Nanoradians)
300 360 55 115 175
1980 1981 Day number
N D J F M A M J

Figure 13

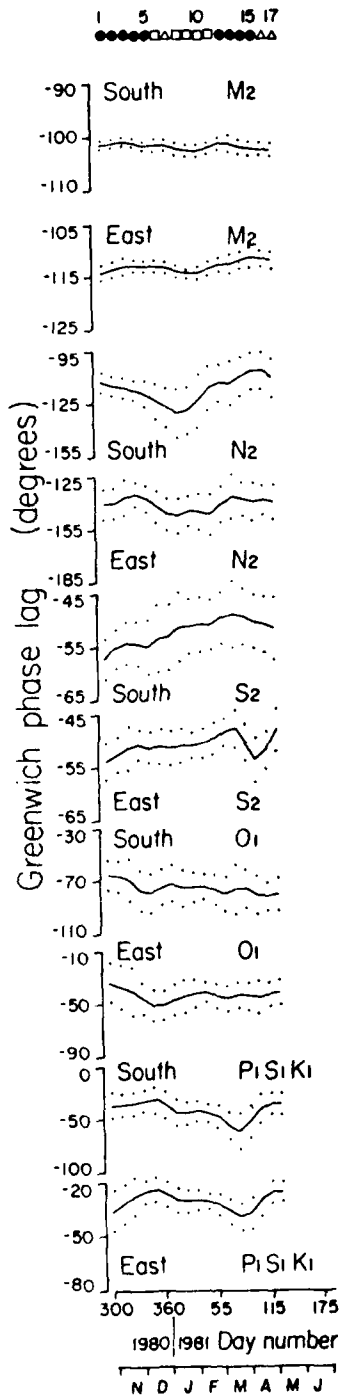
1 5 10 15 17
Greenwich phase lag (degrees)
-90
-100
-110
South M2
-105
-115
-125
East M2
-95
-125
-155
South N2
-125
-155
-185
East N2
-45
-55
-65
South S2
-45
-55
-65
East S2
-30
-70
-110
South O1
-10
-50
-90
East O1
0
-50
-100
South P1 S1 K1
-20
-50
-80
East P1 S1 K1
300 360 55 115 175
1980 1981 Day number
N D J F M A M J

Figure 14

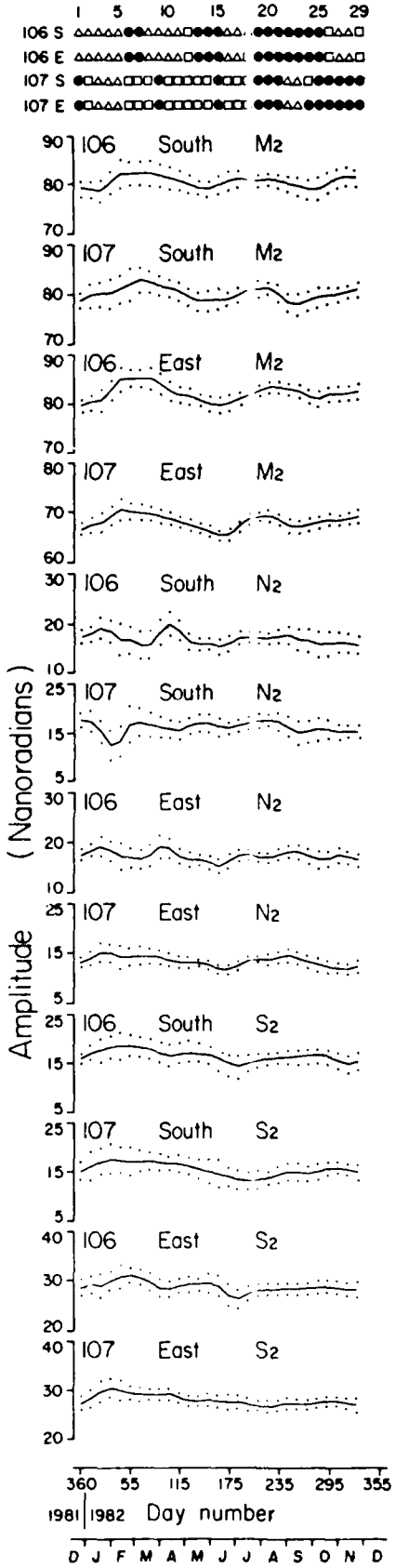
1 5 10 15 20 25 29
106 S
106 E
107 S
107 E
106 South M2
107 South M2
106 East M2
107 East M2
106 South N2
107 South N2
106 East N2
107 East N2
106 South S2
107 South S2
106 East S2
107 East S2
Amplitude (Nanoradians)
360 55 115 175 235 295 355
1981 1982 Day number
D J F M A M J J A S O N D

Figure 15

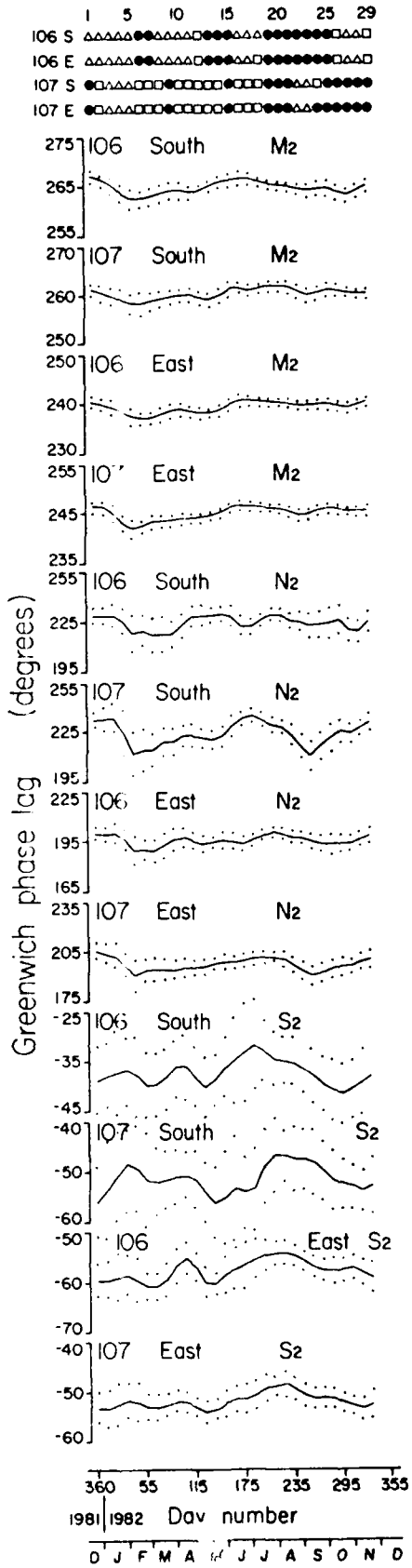
1 5 10 15 20 25 29
106 S
106 E
107 S
107 E
Greenwich phase lag (degrees)
106 South M2
107 South M2
106 East M2
107 East M2
106 South N2
107 South N2
106 East N2
107 East N2
106 South S2
107 South S2
106 East S2
107 East S2
360 55 115 175 235 295 355
1981 1982 Day number
D J F M A M J J A S O N D

Figure 16

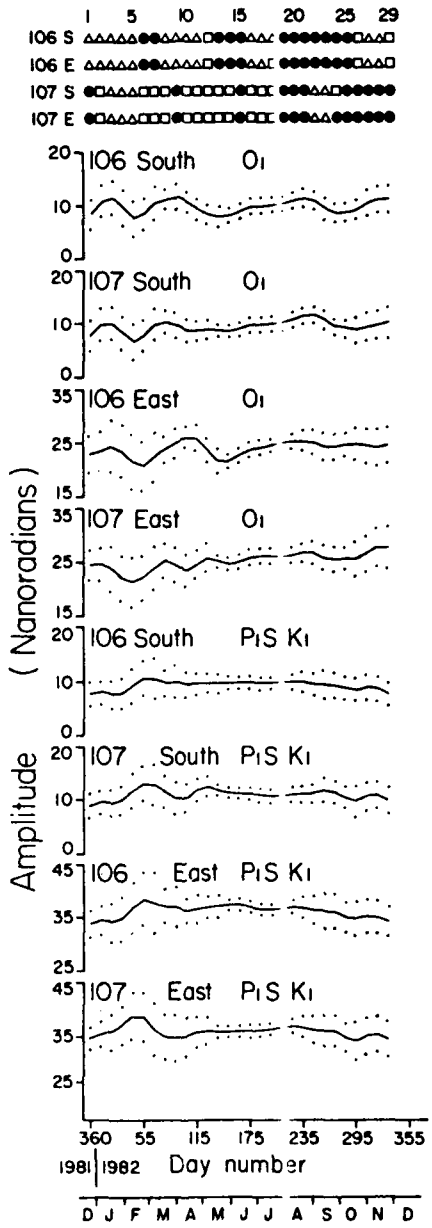
1 5 10 15 20 25 29
106 S
106 E
107 S
107 E
106 South O1
107 South O1
106 East O1
107 East O1
106 South P1S K1
107 South P1S K1
106 East P1S K1
107 East P1S K1
Amplitude (Nanoradians)
360 55 115 175 235 295 355
1981 1982 Day number
D J F M A M J J A S O N D

Figure 17

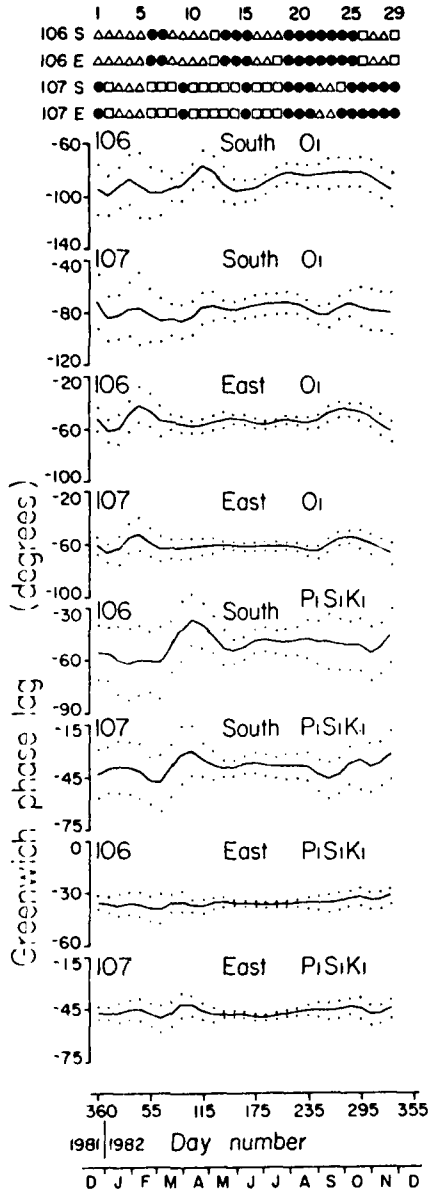
1 5 10 15 20 25 29
106 S
106 E
107 S
107 E
106 South O1
107 South O1
106 East O1
107 East O1
106 South P1S1K1
107 South P1S1K1
106 East P1S1K1
107 East P1S1K1
Greenwich phase lag (degrees)
360 55 115 175 235 295 355
1981 1982 Day number
D J F M A M J J A S O N D

Figure 18

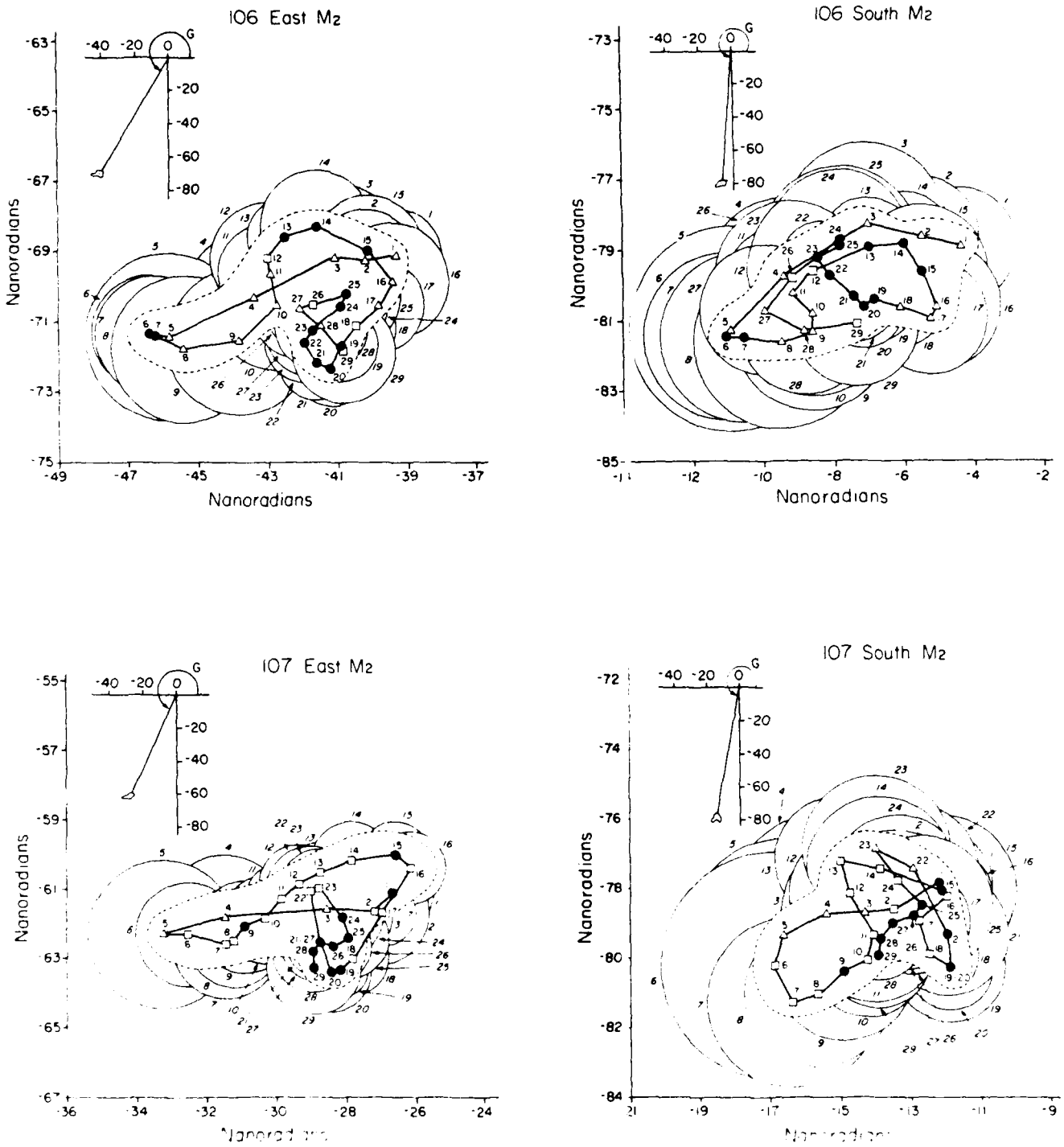
106 East M2
106 South M2
107 East M2
107 South M2
Nanoradians
Nanoradians
G

Figure 19

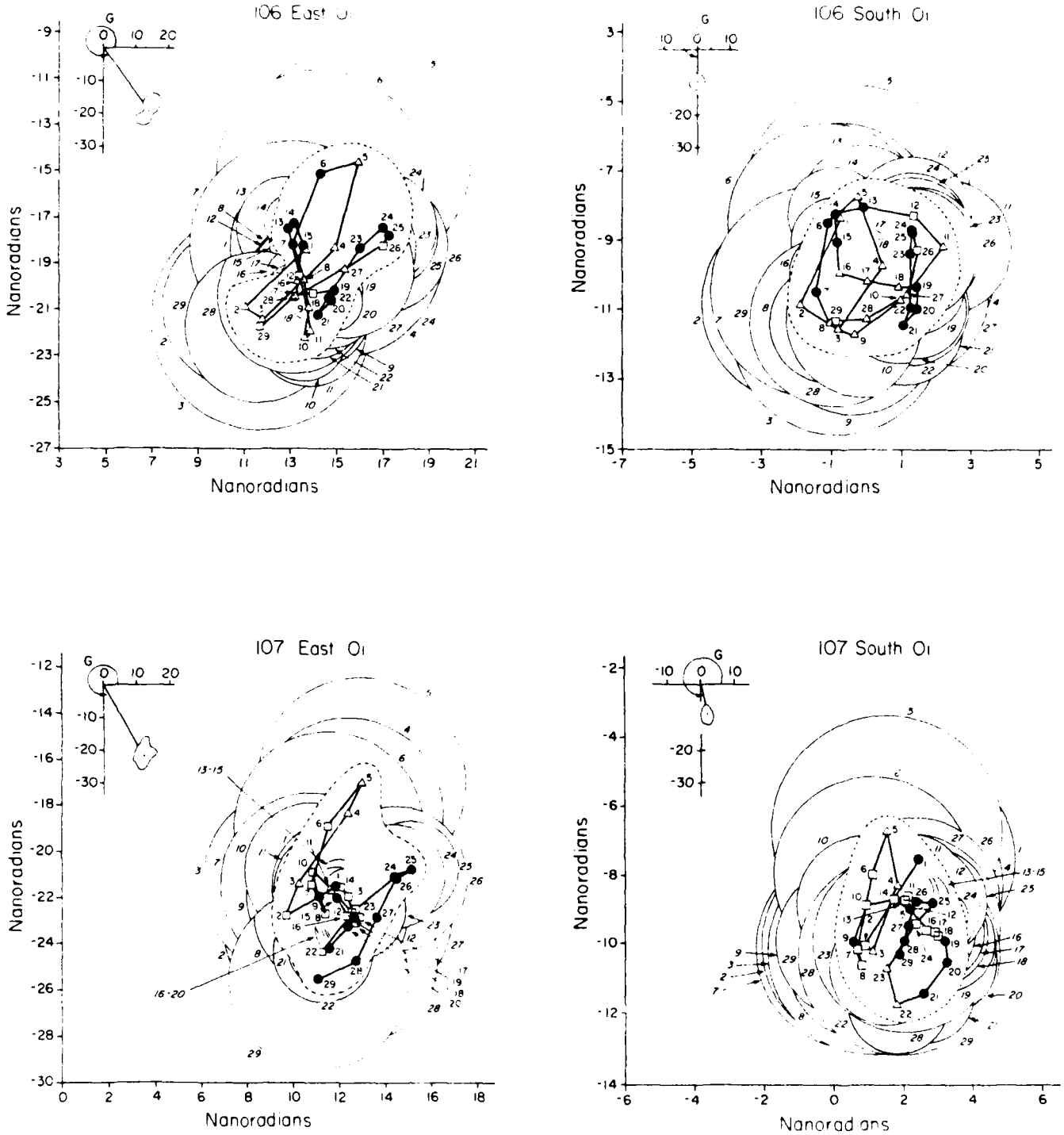
106 East O1
106 South O1
107 East O1
107 South O1
Nanoradians
Nanoradians

Figure 20

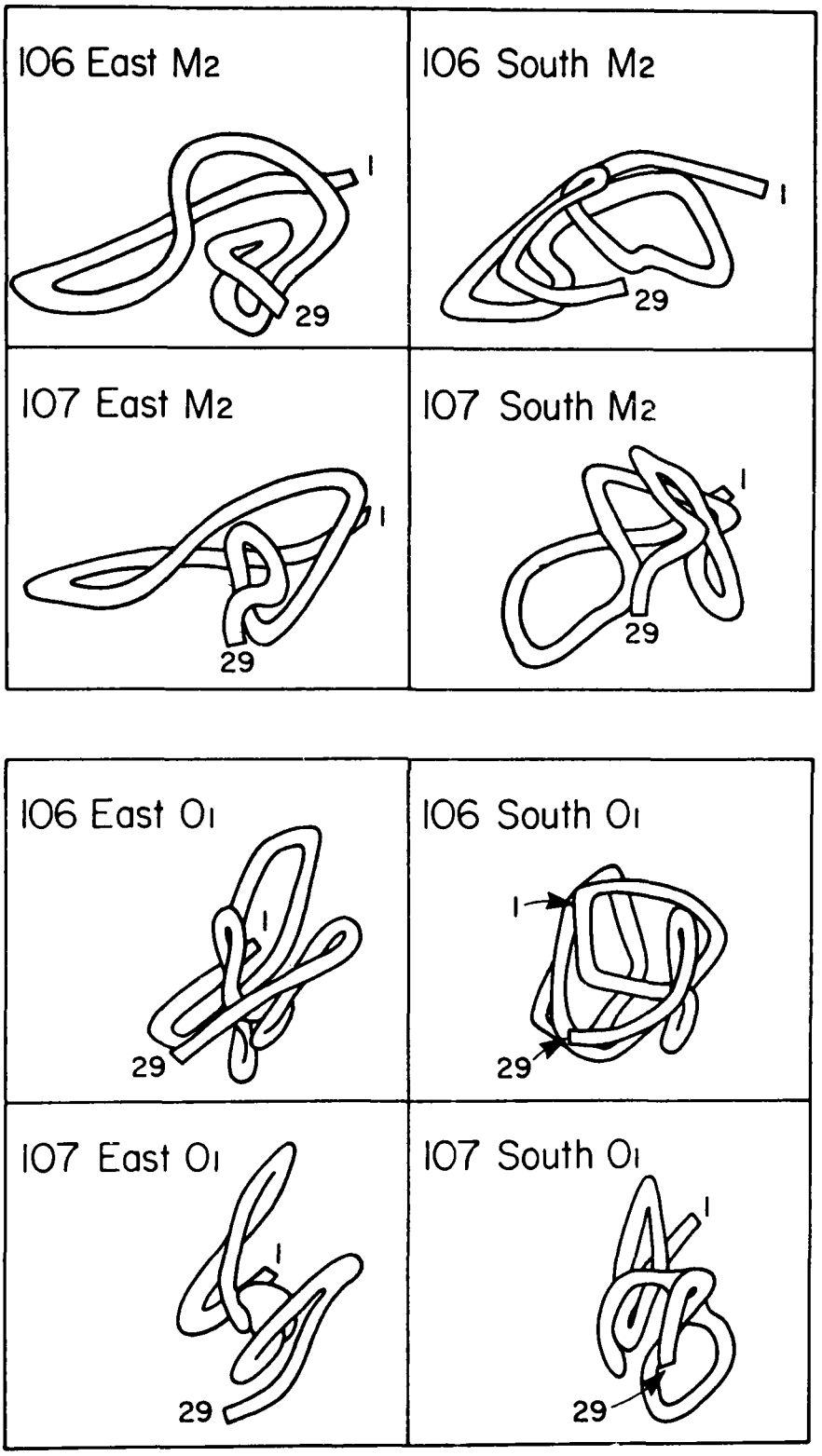
106 East M2
1
29
106 South M2
1
29
107 East M2
1
29
107 South M2
1
29
106 East O1
1
29
106 South O1
1
29
107 East O1
1
29
107 South O1
1
29

Figure 21

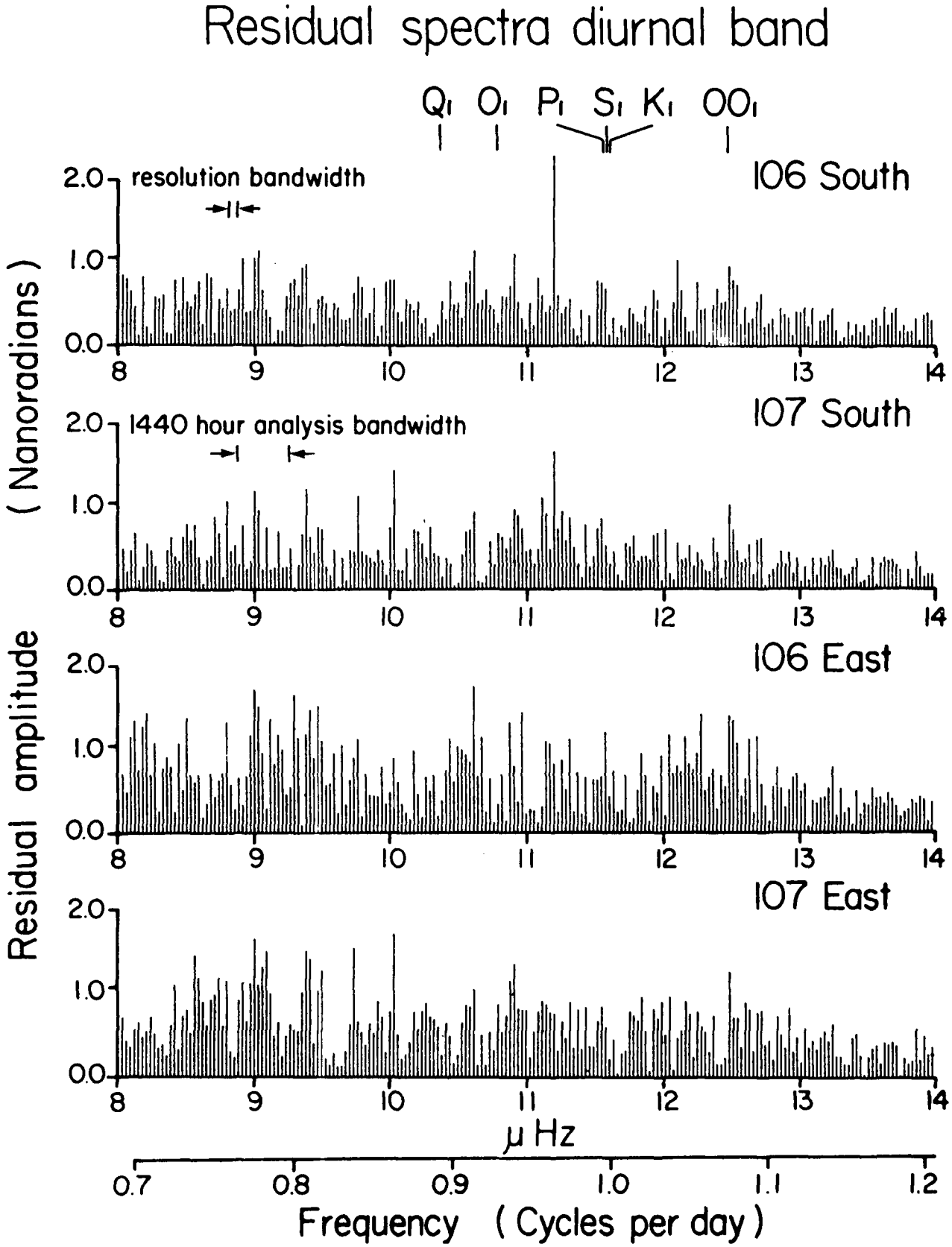
Residual spectra diurnal band
Q1 O1 P1 S1 K1 OO1
resolution bandwidth
106 South
1440 hour analysis bandwidth
107 South
106 East
107 East
Residual amplitude (Nanoradians)
2.0
1.0
0.0
8 9 10 11 12 13 14
μ Hz
0.7 0.8 0.9 1.0 1.1 1.2
Frequency (Cycles per day)

Figure 22

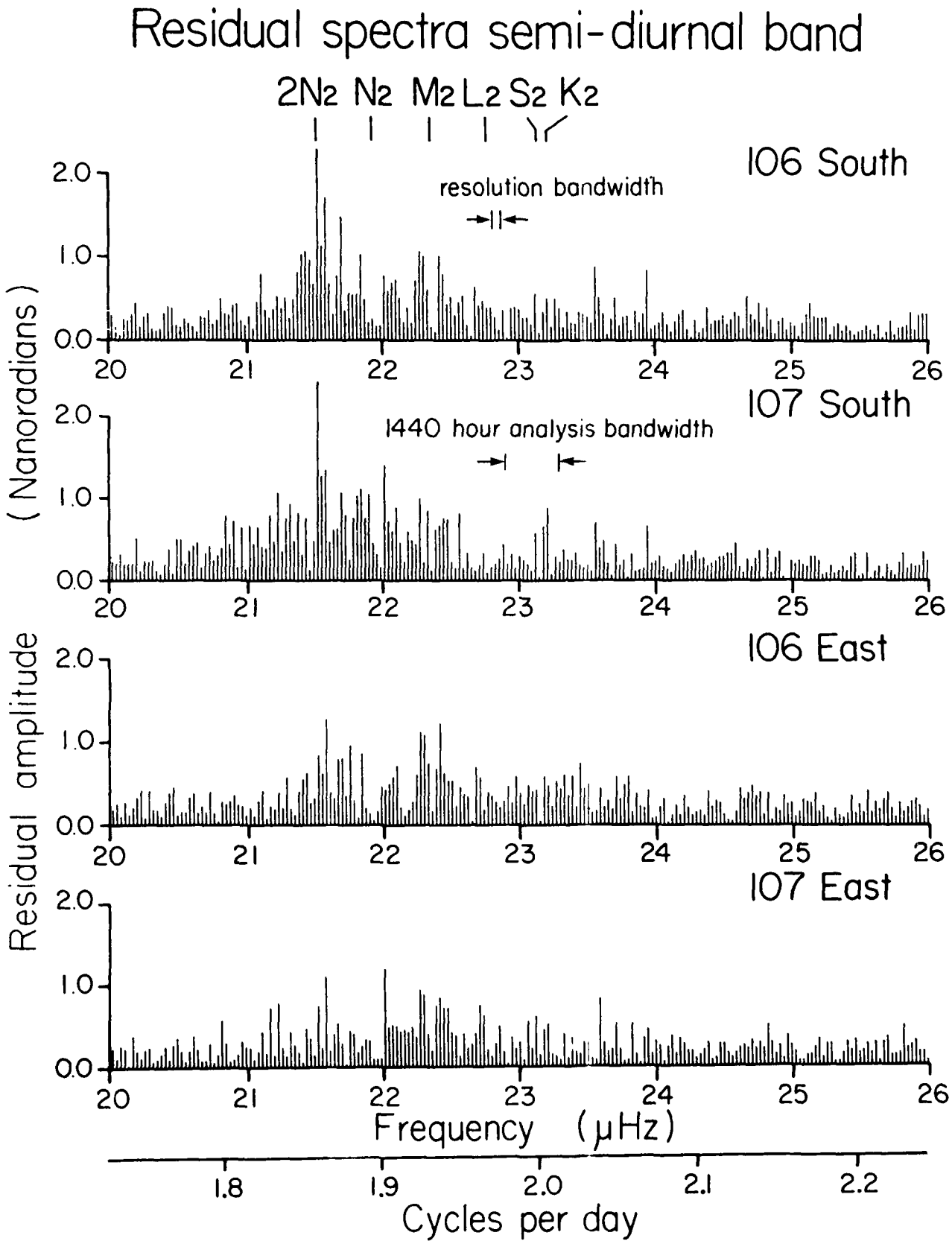
Residual spectra semi-diurnal band
2N2 N2 M2 L2 S2 K2
106 South
resolution bandwidth
107 South
1440 hour analysis bandwidth
106 East
107 East
Residual amplitude (Nanoradians)
2.0
1.0
0.0
20
21
22
23
24
25
26
Frequency (μHz)
1.8
1.9
2.0
2.1
2.2
Cycles per day

Figure 23

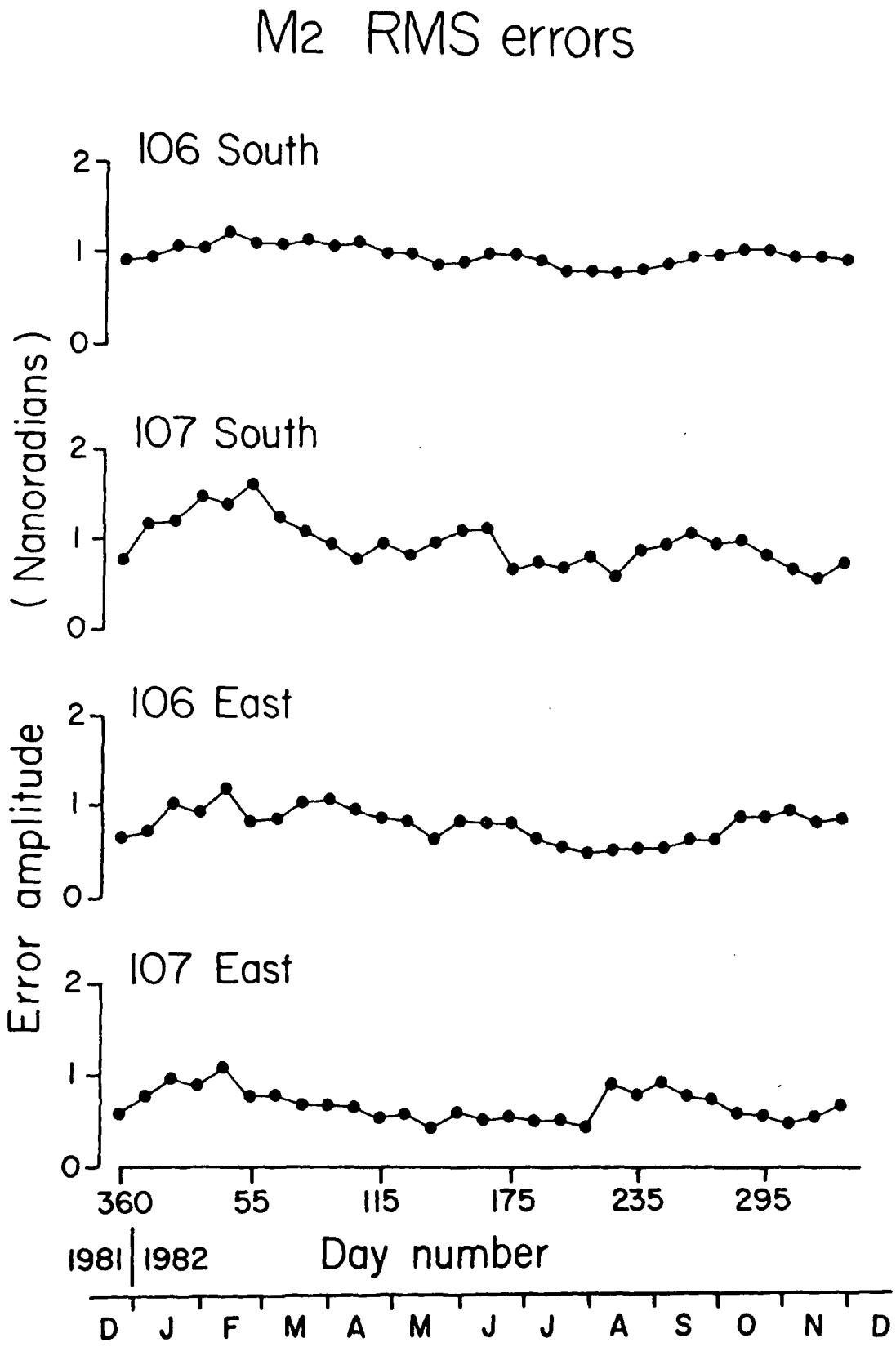
M2 RMS errors
106 South
107 South
106 East
107 East
Error amplitude
(Nanoradians)
2
1
0
360
55
115
175
235
295
1981
1982
Day number
D
J
F
M
A
M
J
J
A
S
O
N
D

Figure 24

END

FILMED

7-85

DTIC